

AD-A064 847

ELECTRONIC VISION CO SAN DIEGO CA
ICCD ELECTRON DAMAGE INVESTIGATION. (U)
JUL 78 R GINAVEN, G HALL, L ACTON

F/6 17/8

UNCLASSIFIED

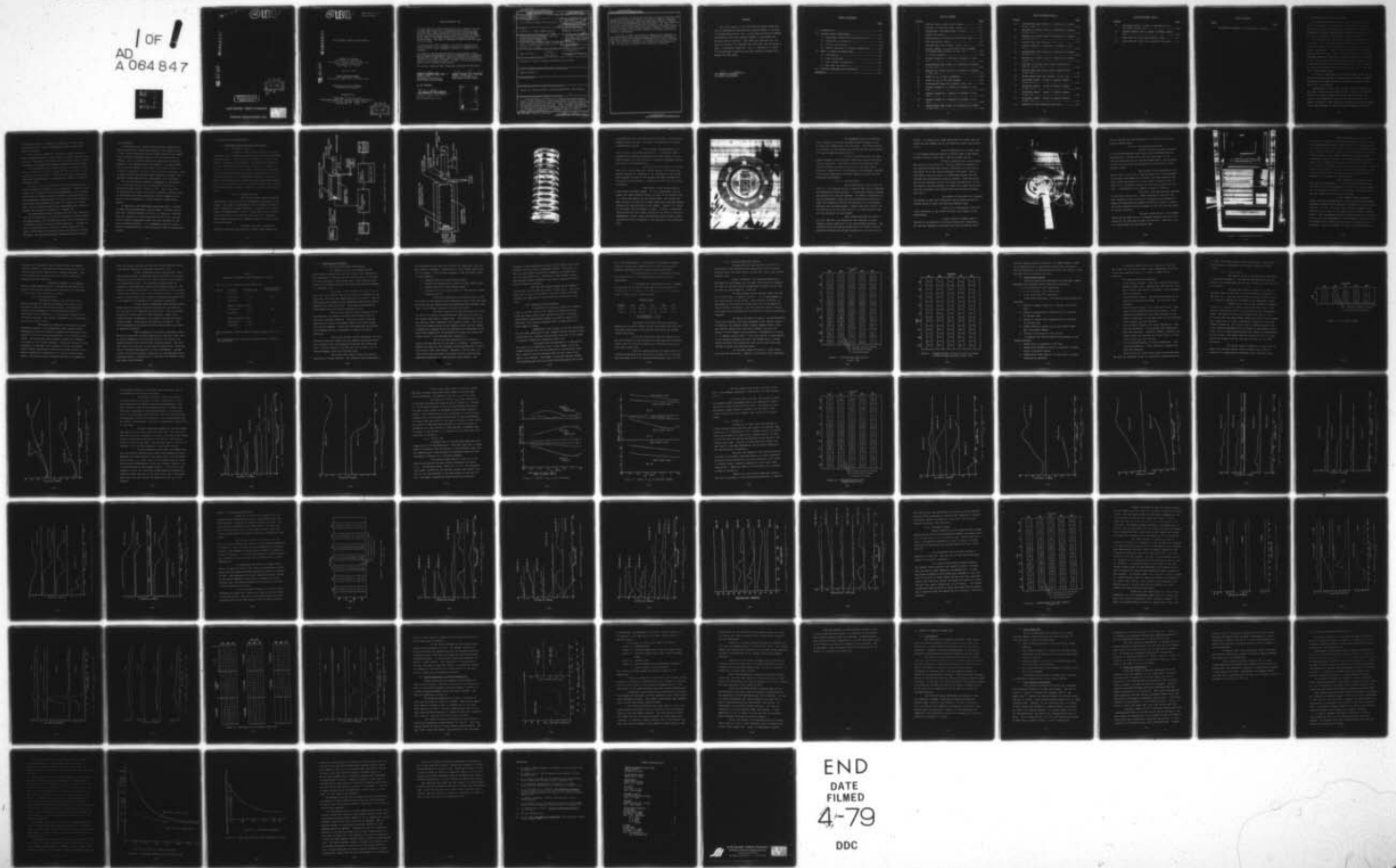
SAI-78-788-EVC

SAMSO-TR-79-2

F04701-76-C-0123

NL

1 OF 1
AD
A 064 847



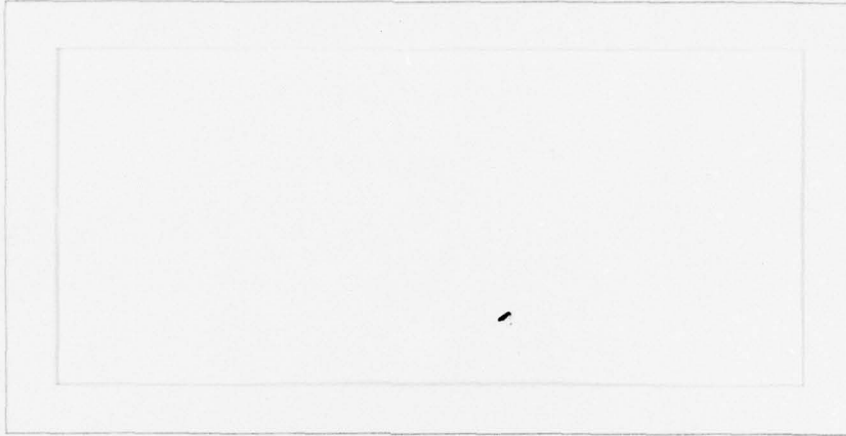
END
DATE
FILMED
4-79
DDC

SHR 50-TR-79-2

12

LEVEL II

ADA 064847



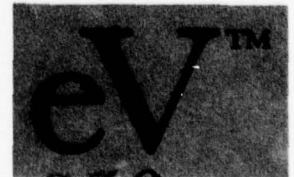
DDC FILE COPY

DDC
RECEIVED
FEB 23 1979
B

DISTRIBUTION STATEMENT A
Approved for public release;
Distribution Unlimited

ELECTRONIC VISION COMPANY

SCIENCE APPLICATIONS, INC.



79 02 16 050

12 LEVEL II

SAMSO TR NO. 79-2

SAI-78-788-EVC

ADA064847

ICCD ELECTRON DAMAGE INVESTIGATION

Robert O. Ginaven
Electronic Vision Company
A Division of Science Applications, Inc.
11526 Sorrento Valley Road
San Diego, CA 92121

July 24, 1978

FINAL TECHNICAL REPORT

For Period 1 April 1977 - 24 July 1978

Approved For Public Release;
Distribution Unlimited

Prepared For:

Department of the Air Force
Headquarters Space and Missile Systems Organization
P.O. Box 92960, Worldway Postal Center
Los Angeles, CA 90009

DDC FILE COPY

DDC
RECEIVED
FEB 23 1979
B

79 02 16 050


REVIEW AND APPROVAL PAGE

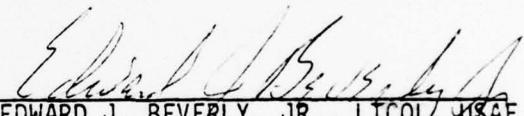
This final report was submitted by Electronic Vision Company, a division of Science Applications, Inc., 11526 Sorrento Valley Road, San Diego, California 92121, under contract F04701-76-C-0123 with the Department of the Air Force, Hq Space and Missile Systems Organization (Hq SAMSO) (AFSC), Space Defense Systems Program Office (YN), Directorate of Survivability (YNV), P.O. Box 92960, Worldway Postal Center, Los Angeles, California 90009. Capt Joseph E. Hernandez, HQ SAMSO/YNV was the Project Officer in charge.

The views and conclusions contained in this document are those of the authors and should not be interpreted as necessarily representing the official policies, either expressed or implied, of Hq SAMSO or the U.S. Government.


This report has been reviewed and cleared for open publication and/or public release by the appropriate Office of Information (OI) in accordance with AFR 190-17 and DODD 5230.9. There is no objection to unlimited distribution of this report to the public at large, or by DDC to the National Technical Information Service (NTIS). At NTIS it will be available to the general public, including foreign nationals.

This technical report has been reviewed and is approved for publication.


JOSEPH E. HERNANDEZ, CAPT, USAF
Project Officer
Directorate of Survivability
Space Defense Systems Program


EDWARD J. BEVERLY, JR., LTCOL, USAF
Director of Survivability
Space Defense Systems Program

FOR THE COMMANDER


RICHARD G. DINGMAN, Colonel, USAF
Assistant Program Director
Space Defense Systems Program

ACCESSION for	
NTIS	Write Section <input checked="" type="checkbox"/>
DDC	Buff Section <input type="checkbox"/>
UNANNOUNCED	<input type="checkbox"/>
JUSTIFICATION	
BY	
DISTRIBUTION/AVAILABILITY CODES	
Dist.	or SPECIAL
A	

Unclassified

SECURITY CLASSIFICATION OF THIS PAGE (When Data Entered)

REPORT DOCUMENTATION PAGE		READ INSTRUCTIONS BEFORE COMPLETING FORM
1. REPORT NUMBER 18 SAMSQ TR NO 79-2	2. GOVT ACCESSION NO.	3. RECIPIENT'S CATALOG NUMBER
4. TITLE (and Subtitle) 6 ICCD Electron Damage Investigation.		5. TYPE OF REPORT & PERIOD COVERED 9 Final Report, 1 April 1977 - 24 July 1978
7. AUTHOR(s) 10 R. Ginaven, G. Hall, and L. Acton		6. PERFORMING ORG. REPORT NUMBER SAI-78-788-EVC
		8. CONTRACT OR GRANT NUMBER(s) 15 F04701-76-C-0123 <i>new</i>
9. PERFORMING ORGANIZATION NAME AND ADDRESS Electronic Vision Company, A Div. of Science Applications, Inc. 11526 Sorrento Valley Road San Diego, CA 92121		10. PROGRAM ELEMENT, PROJECT, AREA & WORK UNIT NUMBERS 16 PE63438F, Proj. 2132 & 2133, Work Unit #DE 368201
11. CONTROLLING OFFICE NAME AND ADDRESS Dept. of The Air Force, Hq. SAMSQ (AFSC)/YINV, P.O. BOX 92960, Worldway Postal Center, Los Angeles, CA 90009		12. REPORT DATE 11 24 July 1978
14. MONITORING AGENCY NAME & ADDRESS (if different from Controlling Office) Same as Block 11		13. NUMBER OF PAGES 76
		15. SECURITY CLASS. (of this report) Unclassified
		15a. DECLASSIFICATION/DOWNGRADING SCHEDULE
16. DISTRIBUTION STATEMENT (of this Report) Approved for public release; distribution unlimited.		
17. DISTRIBUTION STATEMENT (of the abstract entered in Block 20, if different from Report) Same as Block 16		
18. SUPPLEMENTARY NOTES		
19. KEY WORDS (Continue on reverse side if necessary and identify by block number) Satellite, optical sensor, charge coupled device, and Digicon.		
20. ABSTRACT (Continue on reverse side if necessary and identify by block number) ➤ The operational lifetime of an Intensified Charge Coupled Device (ICCD) utilizing a front-illuminated Fairchild CCD202 to detect photoelectrons has been evaluated for operating conditions anticipated in space applications. Under electron bombardment, the CCD exhibited severe increases in dark current and reduction in responsivity after detecting approximately 10^6 electrons per pixel, which corresponds to a lifetime of about 10 hours.		

DD FORM 1 JAN 73 1473 EDITION OF 1 NOV 65 IS OBSOLETE

Unclassified 390074
SECURITY CLASSIFICATION OF THIS PAGE (When Data Entered)

Unclassified

SECURITY CLASSIFICATION OF THIS PAGE(When Data Entered)

In an effort to extend the lifetime of front-irradiated CCDs, parametric studies of the effects of electron energy, operating temperature of the CCD, clock voltages, and annealing (thermal, UV, and electron-bombardment) were performed. The only technique which can significantly extend the lifetime of the presently available front-illuminated Fairchild CCD202 type device appears to be to sequentially utilize different segments of the array. Perhaps an order of magnitude increase in lifetime could be obtained in this manner.

A survey of other CCD radiation damage work suggested two techniques which could significantly increase ICCD lifetime. The use of radiation hardening techniques during array fabrication can produce an increase in lifetime of two orders of magnitude, and the use of thinned rear-illuminated CCDs appears to yield an increase of three to four orders of magnitude.

Unclassified

SECURITY CLASSIFICATION OF THIS PAGE(When Data Entered)

FOREWARD

This final report on the ICCD Electron Damage Investigation is submitted by the Electronic Vision Company, a Division of Science Applications, Inc., to the Space and Missile Systems Organization, Air Force Systems Command in accordance with Contract F04701-76-C-0123. The study was conducted over the period from April 1977 through June 1978 under the direction of Capt. J. Hernandez, SAMSO/YNV. Drs. S. Kash and N. C. Chang of the Aerospace Corporation provided technical guidance and support for the study.



Dr. Robert O. Ginaven
Principal Investigator

TABLE OF CONTENTS

	<u>Page</u>
1.0 INTRODUCTION.....	1-1
2.0 ELECTRON DAMAGE MEASUREMENTS.....	2-1
2.1 Measurement System and Array Description.....	2-1
2.2 Experimental Procedures.....	2-16
2.3 Electron Beam Damage.....	2-23
2.4 Thermal Annealing of Electron Damaged CCD.....	2-59
3.0 SURVEY OF OTHER CCD DAMAGE DATA.....	3-1
3.1 Introduction.....	3-1
3.2 Basic Mechanisms.....	3-2
3.3 Front Surface Illumination.....	3-2
3.4 Back Side Illumination.....	3-3
4.0 LIFETIME ASSESSMENT AND CONCLUSIONS.....	4-1
REFERENCES.....	5-1

LIST OF FIGURES

<u>Figure</u>		<u>Page</u>
1	ELECTRON DAMAGE SYSTEM BLOCK DIAGRAM.....	2-2
2	SCHEMATIC OF ELECTRON DAMAGE SYSTEM.....	2-3
3	CONVENTIONAL "NON-DEMOUNTABLE" DIGICON.....	2-4
4	HEADER WITH CCD202.....	2-6
5	MICROPROJECTOR POSITIONING WITH DIGICON TUBE.....	2-9
6	DATA ACQUISITION SYSTEM.....	2-11
7	ELECTRON BEAM SPOT CONTOUR: 18 keV, 25°C.....	2-21
8	LEAKAGE CURRENT (IN DIGITAL UNITS PER 10 FRAMES) AT ELECTRON BEAM LOCATION; 18 keV, 25°C.....	2-22
9	15 kV SPOT CONTOUR.....	2-26
10	LEAKAGE CURRENT AS A FUNCTION OF FLUENCE; 15 keV, 25°C.....	2-27
11	PHOTOELECTRON BEAM SIGNAL AS A FUNCTION OF FLUENCE; 15 keV, 25°C.....	2-29
12	RESPONSE TO VISIBLE LIGHT AS A FUNCTION OF FLUENCE; 15 keV, 25°C.....	2-30
13	EFFECT OF ϕ_{PL} ON TEST PARAMETERS.....	2-32
14	EFFECT OF ϕ_{PL} ON CCD DARK CURRENT.....	2-33
15	PHOTOELECTRON BEAM SPOT CONTOUR 18 keV, 25°C.....	2-35
16	LEAKAGE CURRENT AS A FUNCTION OF FLUENCE; 18 keV, 25°C.....	2-36
17	LEAKAGE CURRENT AS A FUNCTION OF FLUENCE; 18 keV, 25°C.....	2-37
18	LEAKAGE CURRENT AS A FUNCTION OF FLUENCE; 18 keV, 25°C.....	2-38
19	PHOTOELECTRON BEAM SIGNAL AS A FUNCTION OF FLUENCE; 18 keV, 25°C.....	2-39

LIST OF FIGURES (Cont.)

<u>Figure</u>		<u>Page</u>
20	PHOTOELECTRON BEAM SIGNAL AS A FUNCTION OF FLUENCE; 18 keV, 25°C.....	2-40
21	RESPONSE TO VISIBLE LIGHT AS A FUNCTION OF FLUENCE; 18 keV, 25°C.....	2-41
22	RESPONSE TO VISIBLE LIGHT AS A FUNCTION OF FLUENCE; 18 keV, 25°C.....	2-42
23	ELECTRON BEAM SPOT CONTOUR; 18 keV, 0°C.....	2-44
24	LEAKAGE CURRENT AS A FUNCTION OF FLUENCE; 18 keV, 0°C.....	2-45
25	PHOTOELECTRON BEAM SIGNAL AS A FUNCTION OF FLUENCE; 18 keV, 0°C.....	2-46
26	RESPONSE TO VISIBLE LIGHT AS A FUNCTION OF FLUENCE; 18 keV, 0°C.....	2-47
27	RESPONSE TO VISIBLE LIGHT ACROSS ELECTRON SPOT, LINE 59; 18 keV, 0°C.....	2-48
28	PHOTOELECTRON BEAM SIGNAL ACROSS ELECTRON SPOT; 18 keV, 0°C.....	2-49
29	PHOTOELECTRON BEAM SPOT CONTOUR; 18 keV, 25°C.....	2-51
30	COLLATERAL DAMAGE: COLUMN 65 LEAKAGE CURRENT; 18 keV, 0°C.....	2-53
31	COLLATERAL DAMAGE: COLUMN 66 LEAKAGE CURRENT; 18 keV, 0°C.....	2-54
32	COLLATERAL DAMAGE: COLUMN 67 LEAKAGE CURRENT; 18 keV, 0°C.....	2-55
33	COLLATERAL DAMAGE: COLUMN 68 LEAKAGE CURRENT; 18 keV, 0°C.....	2-56
34	VARIATION OF SPOT CONTOUR DURING TEST.....	2-57

LIST OF FIGURES (Cont.)

<u>Figure</u>		<u>Page</u>
35	COLLATERAL DAMAGE: COLUMN 66 RESPONSE TO VISIBLE LIGHT; 18 keV, 0°C.....	2-58
36	LEAKAGE CURRENT LINE 54 EFFECT OF THERMAL ANNEALING.....	2-60
37	COUNT RATE PER PIXEL FROM ZODIACAL LIGHT.....	4-3
38	COUNT RATE PER PIXEL FROM INTEGRATED STARLIGHT....	4-4

LIST OF TABLES

Table

Page

1 THICKNESS OF MATERIAL OVER PHOTOSITES IN CCD202.... 2-15

1.0 INTRODUCTION AND EXECUTIVE SUMMARY

The Intensified Charge Coupled Device (ICCD) has the potential of becoming a very attractive detector for many space applications due to its extremely high sensitivity, small size, ruggedness, low power requirements, absence of lag and suitability for use with a digital data processing system.

The ICCD utilizes a CCD array to detect electrons which are emitted from a photocathode, accelerated by an electric field and imaged onto the CCD which is inside the vacuum tube. Actual measurements with an ICCD demonstrated single photoelectron detection with a high signal-to-noise ratio. However, prolonged exposure of the CCD to electrons from the front side of the array produced severe degradation of CCD performance (increased dark current and decreased sensitivity). The lifetime of the ICCD was identified as a critical issue and is the subject of the present study.

In order to understand the electron-induced damage and investigate possible methods of extending the lifetime, extensive measurements have been carried out using the Fairchild CCD202 array (100 x 100 pixels).

Measurements of pixel dark current, electron sensitivity, and light sensitivity have been made as a function of electron fluence at electron energies of 18 keV and 15 keV with the array at room temperature and at 18 keV with the array at 0°C. Severe increases in dark current and reduction in electron sensitivity were observed at electron fluences between 10^6 and 10^7

electrons per pixel. In addition to damage to pixels within the electron spot, vertical streaking occurred at very high electron fluences.

In an effort to extend the lifetime of front irradiated CCDs, parameter studies of the effects of electron energy, temperature of operation of the ICCD, clock voltages, pixel to pixel variations, and thermal and radiation annealing were performed.

Even though there were slight trends in the amount of damage as a function of electron energy (15 keV vs. 18 keV), temperature of the array (0-25°C), and clock voltages, the improvements were insignificant in extending the lifetime of the front irradiated ICCD.

In order to try to alleviate the electron-induced damage, several methods of annealing were investigated: thermal, ultraviolet (UV) radiation, and electron-bombardment. Some recovery was achieved by thermal annealing; however, prolonged baking at high temperature (approximately 4 hours at 300°C) was necessary. This method does not appear practical for recovery of an ICCD tube. The UV radiation and electron bombardment were unable to produce any significant recovery of a damaged CCD.

The measurement program indicated that the total photoelectron count capability of the front-illuminated Fairchild CCD202 was approximately 10^6 electrons per pixel, which corresponds to a lifetime of about 10 hours in normal operation. Viewing the sky in close proximity to the sun or direct viewing of the moon or earth would significantly reduce the detector lifetime. Obviously, any sensitive detector should be protected against

such exposures.

The present study indicates that the only technique that could significantly extend the lifetime of the present version of the front-illuminated Fairchild CCD202 appears to be sequentially utilizing different areas of the CCD as the array is damaged. This is possible because no significant horizontal blooming of the damaged region was observed. By using different horizontal segments of the array, the lifetime could be extended by possibly a factor of ten for normal operations. Also, it would preclude the detector being blinded by a single overexposure, except when the last good segment is in operation.

The use of radiation hardening techniques in the fabrication of the array may be able to extend the lifetime of a front-illuminated CCD by a factor of 100. While this effect is insufficient by itself to produce an adequate lifetime, used in conjunction with other techniques (such as segmenting the array or rear illumination) it would provide an added safety margin.

In addition to the measurements described above, a survey of other electron-bombardment data was made. The most significant data, although somewhat difficult to interpret, indicated that the lifetime of a rear-illuminated TI 100 x 160 array may be four orders of magnitude longer than that observed for the front-illuminated CCD202. It is recommended that the availability and applicability of rear-illuminated CCDs be investigated further.

2.0 ELECTRON DAMAGE MEASUREMENTS

2.1 Measurement System and Array Description

2.1.1 Measurement System

In order to study electron damage in electron irradiated CCDs, a system was required that produced an electron beam impinging on the CCD which is controlled in energy, flux density, and spatial distribution. The system also must provide for CCD operation and for data collection, analysis, and storage. In this system three major elements can be described: (1) a unique Digicon tube which can be disassembled for access to the CCD array; (2) a microprojector capable of imaging a UV spot of known shape at any position on the Digicon photocathode; and (3) the CCD operating system and microcomputer data handling and storage system. Figure 1 shows the system in block diagram form.

2.1.1.1 Demountable Tube

The SAI/EVC Digicon image intensifier tube design is the basis for the demountable tube used in this system. This tube is approximately 7 cm in diameter and 20 cm long; a schematic is shown in Figure 2. Figure 3 is a conventional "non-demountable" Digicon. Rather than being a permanently sealed device, the tube for this test had a removable photocathode faceplate and a removable header on which the CCD array was mounted.

The body of the tube consists of identical electrode rings sealed to tubular glass spacers and

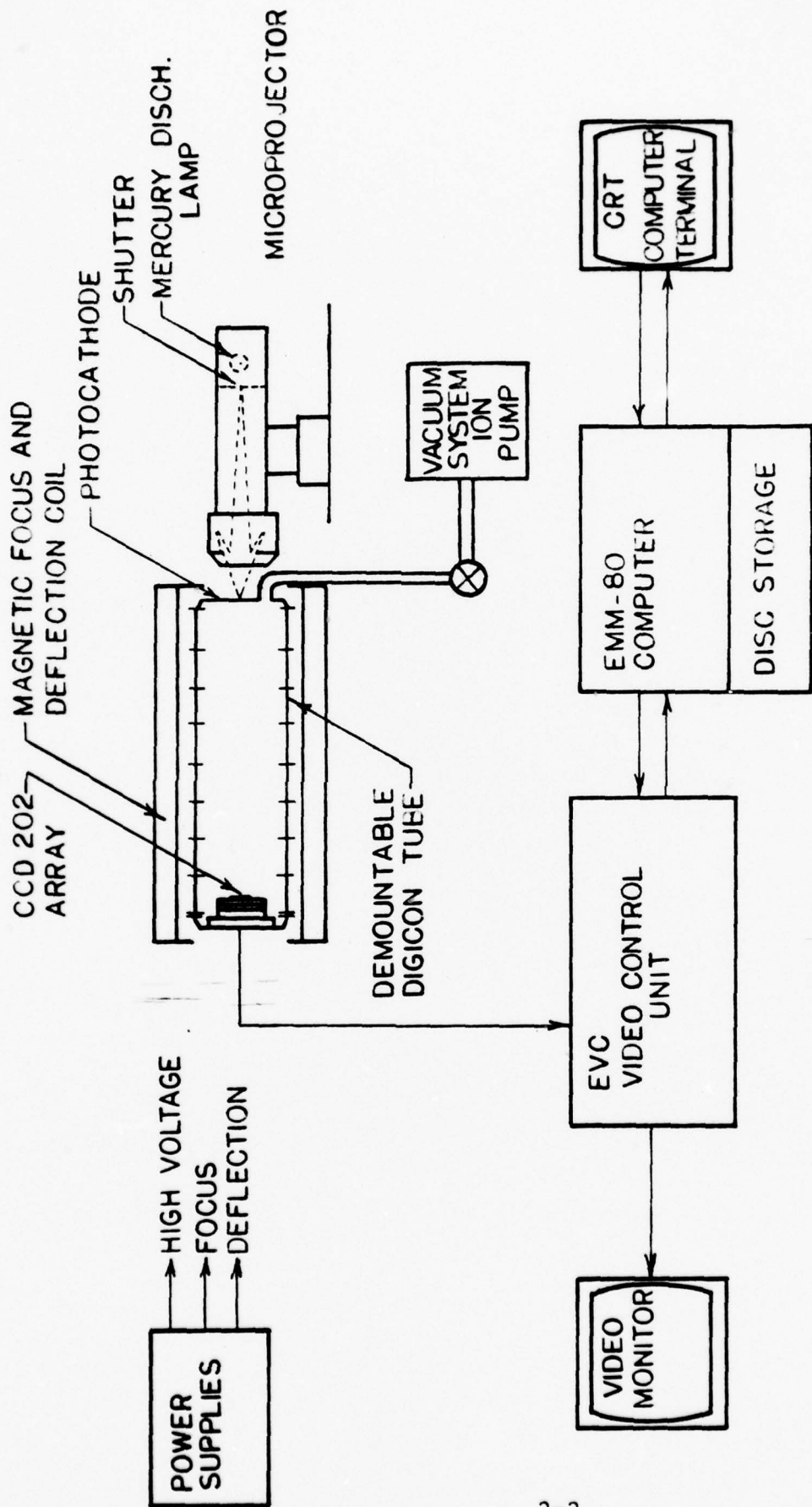


Figure 1. ELECTRON DAMAGE SYSTEM BLOCK DIAGRAM

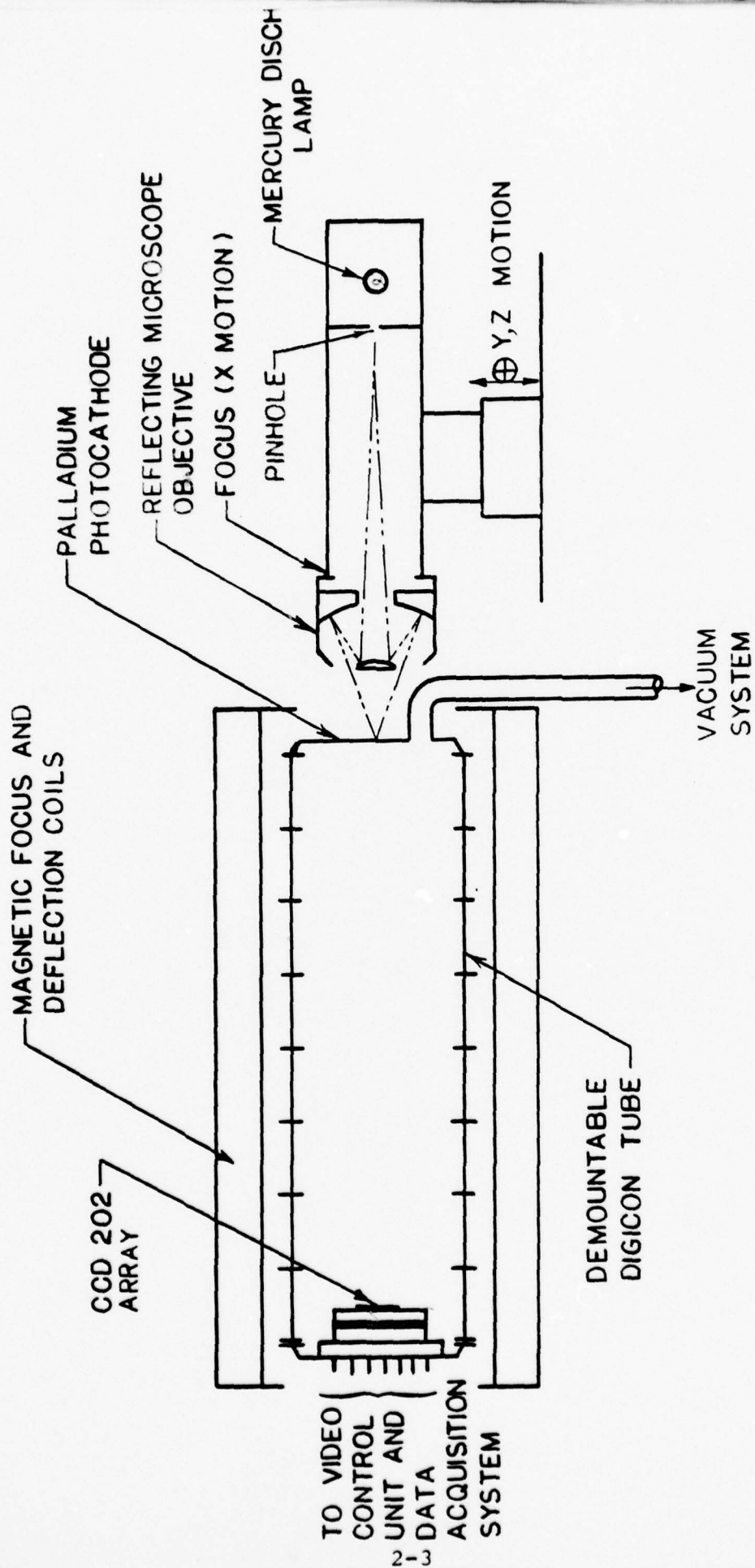


Figure 2. SCHEMATIC OF ELECTRON DAMAGE SYSTEM

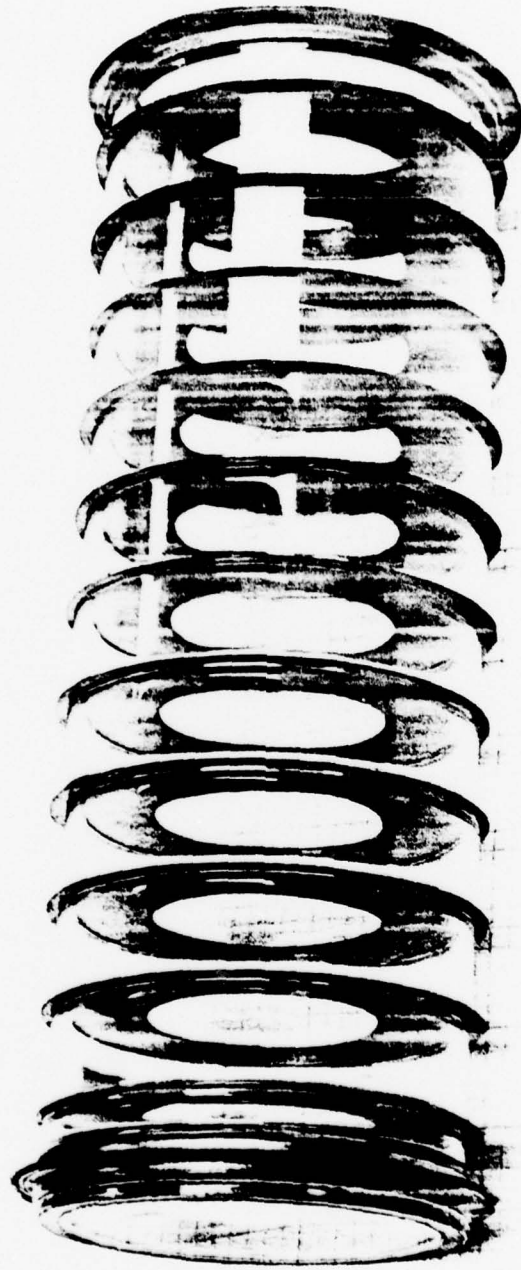


Figure 3. CONVENTIONAL, "NON-DEMOUNTABLE" DIGICON

interconnected with a resistor divider to cause a uniform field gradient along the tube. The tube is encapsulated to prevent interelectrode arcing.

The faceplate has deposited on its inner surface a palladium photocathode. A palladium photocathode can be exposed to ambient air without damage, but the work function (4.97 eV) requires an exciting wavelength shorter than 248 nm for photoemission.

The faceplate is attached to the tube body with a screw clamp and a rubber gasket. The glass tube passing through the faceplate is for attachment to the vacuum pump; because the seal is not perfect the tube is pumped continuously during operation. Pressures of 10^{-6} torr are readily achievable.

The header is also attached with a screw clamp and rubber gasket. It is a conventional Digicon header for linear Reticon arrays; in place of the Reticon array is a 24-pin DIP socket for the CCD202 array. The socket has been cut away to allow for a copper block which provides thermal conductivity from the array to the header. Figure 4 is a photo of the header with the CCD202 in place. In test, a conductive shield covers all but a small portion of the array to provide an unbombarded "virgin" region of photosites and to protect array electronics which are exposed at the periphery of the sensitive area.

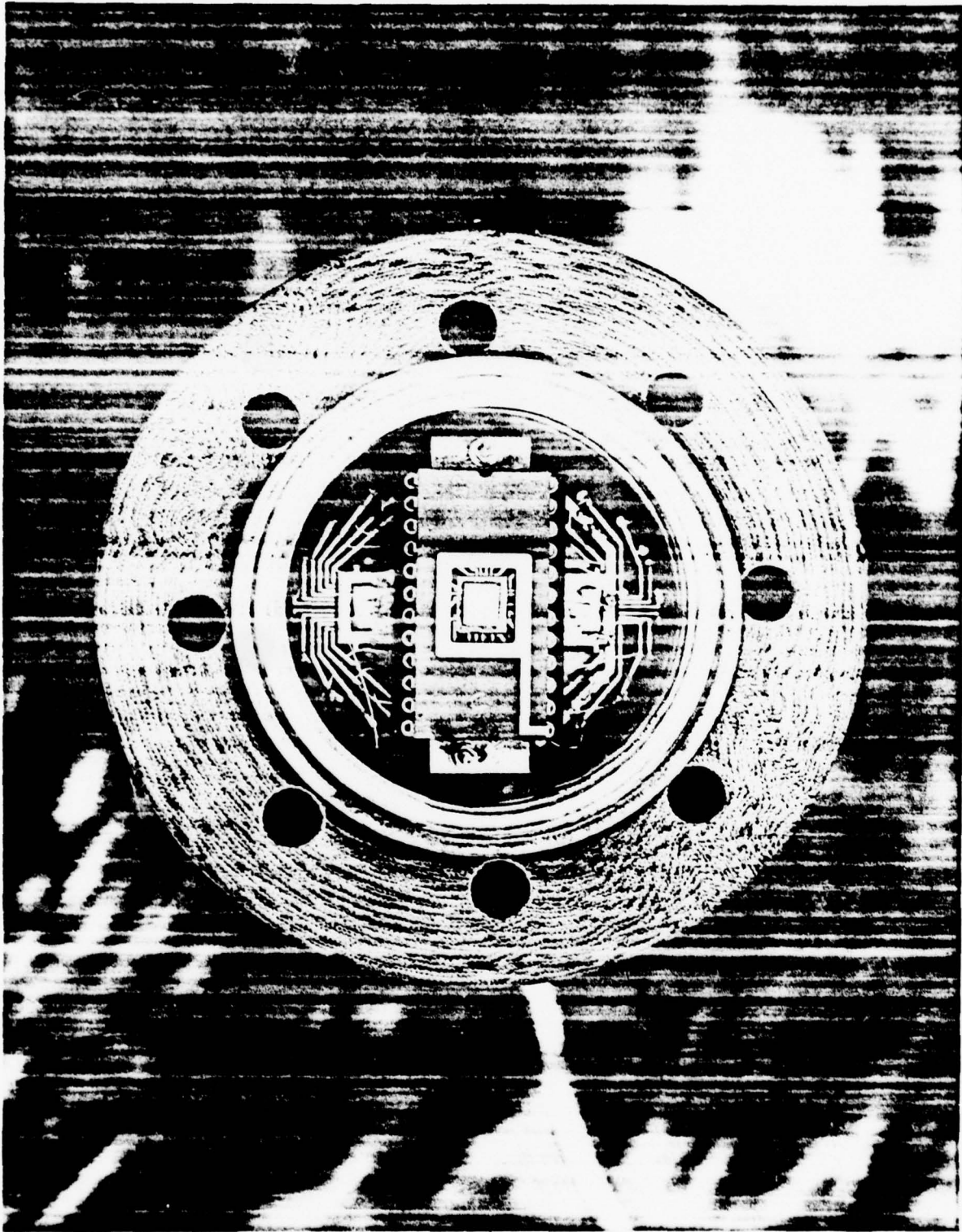


Figure 4. HEADER WITH CCD202

The assembled Digicon is inserted into a solenoid coil which provides an axial magnetic field to focus the cathode image onto the array. The field required is a function of the accelerating voltage and for this solenoid 0.76 amp was used to focus at 18 kV.

A set of deflection coils in quadrature produces a field normal to the axial field to shift the image on the array. This permits moving the electron image without changing the excitation point on the photocathode. Deflection sensitivity is approximately 12 microns/mA. Because of this high sensitivity regulated supplies are used and are monitored continuously.

2.1.1.2 Microprojector

The microprojector light source consists of a low pressure mercury discharge lamp which illuminates and adjustable pinhole aperture. A microscope objective images the aperture onto the photocathode. To achieve transmission of the UV wavelengths a Beck 15X totally-reflecting objective is used; this objective also has the advantage of a long working distance from the photocathode. These objectives, however, do not provide as high an image quality as a glass objective and are very sensitive to misalignment.

Lens systems designed for focus in air will show spherical aberration when required to focus through a quartz plate such as the photocathode substrate. Ray tracing of this lens design showed that this effect could be cancelled by moving the pinhole aperture to 30 cm from the ob-

jective. In practice the image aberrations are larger than expected and are probably due to the objective itself (see Section 2.2.3).

The net magnification is 0.056; thus a 1 mm diameter aperture forms a 56 micron image on the photocathode, slightly larger than a CCD202 transfer region.

Focus is controlled by a fine adjustment device at the objective. The high numerical aperture of the objective ensures that direct illumination of the array is negligible due to the rapid divergence of the beam. This is confirmed by the total lack of an observable signal from the CCD when the accelerating voltage is removed. Rack and pinion motions are provided to shift the entire microprojector to move the image on the photocathode, but these are coarse motions only and fine adjustments are accomplished with the Digicon deflection coils.

The pinhole is provided with a mechanical shutter so that the illumination may be turned on and off without having to start and stop the discharge lamp.

Figure 5 is a photograph of the projector objective at the correct position with respect to the photocathode.

A small tungsten filament lamp is mounted on the objective to provide direct array illumination for the dual purposes of obtaining the array saturation level.

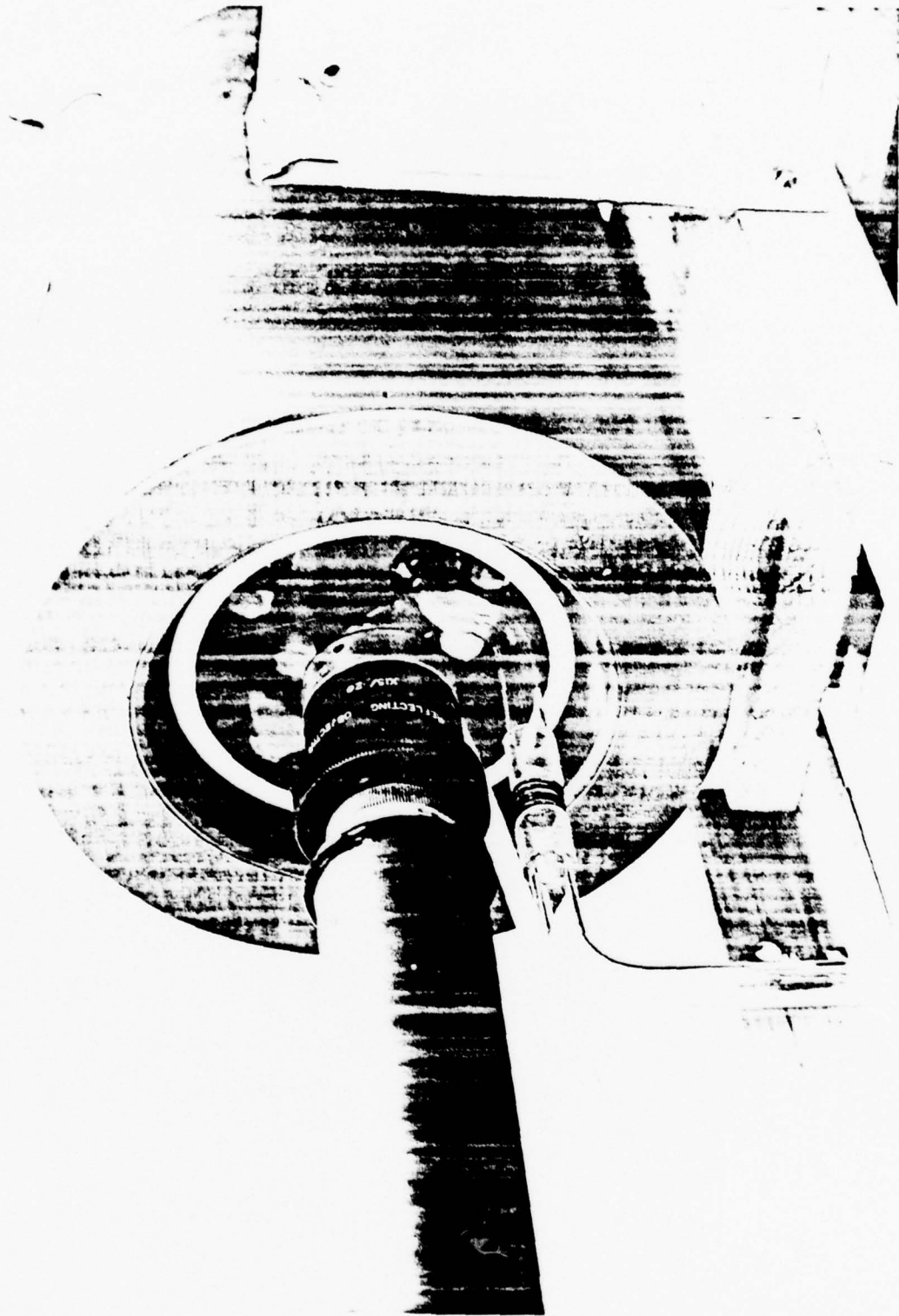


Figure 5. MICROPROJECTOR POSITIONING WITH DIGICON TUBE

and for testing the array sensitivity to visible light during electron damage tests.

2.1.1.3 Data Acquisition System

The data acquisition system consists of the SAI/EVC-designed video control unit and EMM System 80 microcomputer. Modifications have been made based on our previous experience and on the anticipated need in this program for the efficient and rapid manipulation and storage of large amounts of data.

The success of this experimental program is due in large part to the availability of this equipment in providing the capability to record, for later analysis, the simultaneous performance of a large number of pixels, each of which is at a different location on the electron spot flux contour. A photograph of this system is shown in Figure 6.

Only minor modifications were required to the video control unit. These consisted of improving the high frequency signal circuits by increasing the frequency response and improving the impedance matching in order to improve the signal waveform fidelity between the CCD chip and the analog to digital converter.

The major modification to the computer system was the addition of a 5 megabyte magnetic disk drive and controller for mass data storage and retrieval. The disk drive is a Caelus model 8513 provided by EMM.

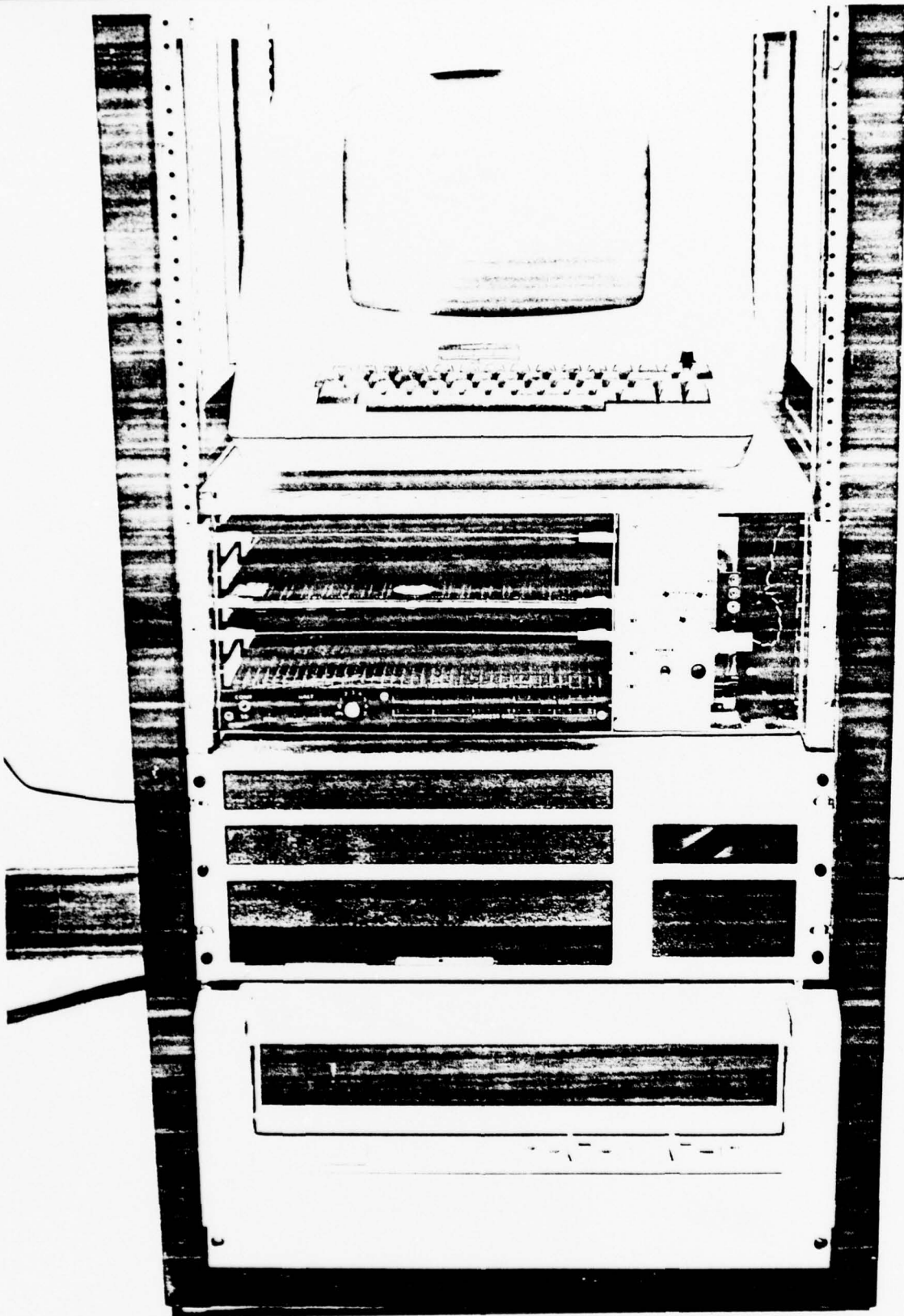


Figure 6. DATA ACQUISITION SYSTEM

WRITE and READ instructions to the disk are now included in our command software, so that as part of a command sequence data can be written to or read from the disk directly into the data buffer blocks of the computer memory. Data retrieved from disk storage can be manipulated by instructions available in our command software or by instructions programmed in BASIC language. For example, during an electron damage test an instruction sequence can be written such that with a single key command the system will input and sum a preset number of data frames, subtract the original background leakage current and write the resulting data array on the disk with a sequential file number for later retrieval.

Frame summation and background subtraction can be performed up to a frame size of 8192 pixels. The system also has the capability of inputting (without summation or background subtraction), writing to, and reading from the disk frame sizes of up to 32,768 pixels.

In the summation mode, successive frames cannot be accepted because of the time required between successive frames for the computer to perform the pixel-by-pixel addition. In this (32K frame) mode successive frames can be accepted up to a total of 32K pixels so as to record transient events. This is possible because the particular array of pixels on the CCD is set independently of the computer frame size, and the computer will accept pixel data until its frame size is satisfied. Thus, for example, an array of 1000 pixels can be

recorded on 32 successive camera frames before one computer frame is completed. The data are stored sequentially on the disk and can be later analyzed for transient phenomena. This mode has been used to obtain data of a target image being scanned across the CCD array.

Additional changes to the computer system include substitution of an LSI-ADM-3A CRT terminal in place of the printing terminal used previously and replacement of core memory with semiconductor memory.

2.1.2 Array Description

The Fairchild CCD202 is a CCD area image sensor providing 10^4 photosites arranged in an array of 100 horizontal lines and 100 vertical columns. The photosites (pixels) have dimensions of 18 μm horizontally and 30 μm vertically and are located on 40 μm horizontal centers and 30 μm vertical centers. The overall dimensions of the image sensing area are 4 mm by 3 mm.

The sequential readout of the pixels is accomplished by transfer of the accumulated pixel charge through photogates into the 100 vertical (column) shift registers, each located in the 22 μm wide space adjacent to its respective pixel column. One horizontal shift register accepts and transports the outputs of the column registers. Electrical clocking of the photogate, the vertical shift registers, and the horizontal output register sequentially delivers the charge packets to the charge integrator for conversion to an analog voltage output signal. The vertical shift registers each have 50 elements but

serve 100 pixels; the data are read out in two sequential interlaced fields comprised of alternate horizontal lines.

In the conventional photon imaging mode, image photons pass through a transparent polycrystalline silicon gate structure and are absorbed in the single crystal silicon producing hole-electron pairs. The resulting photoelectrons are collected in the photosites during the integration period. The amount of charge accumulated is a linear function of the incident illumination intensity and of the integration period. The output signal voltage ranges from a thermally generated background level in the absence of illumination to a maximum at saturation.

In the electron bombardment mode employed during these tests the incident electrons generate one hole-electron pair for each 3.6 eV deposited in the silicon. Gain is realized by the use of high energy (15 keV) electrons. Some of the electron energy is absorbed in the layers overlying the single crystal volume: these layers are tabulated in Table 1. The shift registers are protected from the electron beam by a layer of deposited aluminum.

The performance of the device (saturation level, degree of uniformity of photon sensitivity across the array, etc.) is highly dependent on the voltage values of the positive and negative peaks of the various clock voltages applied. The optimum values vary from unit to unit due to manufacturing tolerances and are adjusted experimentally for best performance. Optimum values of the clock voltages (especially ϕ_p , the photogate clock) have been found in previous work to vary with the degree of electron beam induced damage.

TABLE 1
THICKNESS OF MATERIAL OVER PHOTOSITES IN CCD202

There are three regions over each photosite:

<u>Region*</u>	<u>Material</u>	<u>Thickness (um)</u>	<u>Percent of Area of Photosite</u>
1	Dielectric	0.15	29%
	Polysilicon	0.35	
	Dielectric	0.7	
2	Same as region 1 plus:		34%
	Polysilicon	0.35	
	Dielectric	0.35	
3	Same as region 2 plus:		37%
	Polysilicon	0.35	
	Dielectric	0.35	

Shift registers (vertical) have all above layers plus 1.2 um Al.

*only thicknesses were obtained from manufacturer; geometry not specified.

2.2 Experimental Procedures

2.2.1 Electron Beam Damage Measurements

In a damage test run the leakage current, photoelectron responsivity, and the visible light responsivity were recorded as a function of time for each pixel in an array of pixels centered on the electron spot. Each pixel was subjected to a different electron flux level and therefore damaged at a different rate.

Preliminary setup requires the positioning and focusing of the electron spot on the array at a location on the array away from where the damage data was to be taken. Thus the unavoidable array damage during experiment setup was not superimposed on the later test data. Final spot positioning was accomplished using the Digicon deflection coils.

Also at this time the array saturation level was determined by flooding the array with visible light of controlled variable intensity. This was to verify that the saturation was within the dynamic range of the video control unit and the computer. These data also permitted the analysis of the damage data to be expressed in terms of the array saturation.

The initial leakage current measurement of each monitored pixel was loaded into the computer background buffer. This reference level was subtracted from the data during the test. The data stored on the disk was the variation, due to electron damage, from this reference level.

During the test, sets of data were taken at intervals of several minutes. The intervals were determined by

the experimenter from the rate at which the damage was occurring. The interval, therefore, varied during a test; common values were 2 to 5 minutes. A set of data consisted of the following, taken in rapid sequence:

1. leakage current; UV lamp shutter closed
2. leakage plus photoelectron signal; UV lamp shutter open
3. leakage current; UV lamp shutter closed
4. leakage plus visible lamp signal; UV lamp shutter closed, tungsten lamp on

During data reduction the arithmetic mean of the two values of the leakage current obtained in step 1 and 3 was used. Since the initial leakage value was subtracted from the data, this mean was the leakage caused by the electron fluence.

This mean leakage value was subtracted from data (2) and (4) to obtain the photoelectron responsivity signal and the visible lamp signal, respectively. The photoelectron signal was typically small compared to the leakage current. The variations from frame-to-frame in the leakage current and the leakage increase due to damage during the photoelectron measurement can be significant compared to the photoelectron signal and caused the larger scatter in the photoelectron responsivity.

The UV lamp was operated from a DC source to prevent fluctuations due to the lamp AC frequency. Attempts to operate the lamp at a high frequency were abandoned due to excessive noise on the light output. Operated in the DC mode, the lamp current was monitored continuously and the lamp polarity reversed periodically to reduce the DC aging effects. The

constancy of the photoelectron signal on the medium flux pixels indicates that the lamp is adequately stable. The signal on the high flux pixels varied due to responsivity damage and on the low flux pixels due to variations in the leakage current and the small signal compared to the finite resolution of the analog-to-digital converter.

All data were taken summed over 10 frames of the CCD and all flux data are given in those units. They have been left in units of 10 frames to provide a basis for understanding the magnitude of the statistical uncertainty of the data.

2.2.2 Electron Flux Calibration

To establish the relation between the computer signal in digital units to the number of photoelectrons per pixel per frame, pulse height analysis was used. A separate multi-channel pulse height analyzer was used to examine the amplitude of the video pulseheight from a single pixel for a large number of frames.

Comparison of the outputs of the two instruments for two known conditions of zero (leakage current) and half scale illumination by a tungsten lamp provided the scale of the number of analyzer channels per computer digital unit.

The system was then operated at a sufficiently low level of UV illumination that a large number of the CCD frames contained only one photoelectron on the monitored pixel. This "singles" peak was resolved from the zero signal noise peak in the analyzer. The number of analyzer channels between the background peak and the singles peak represented the signal

due to one photoelectron. Because the correspondence between analyzer channels and computer digital units was previously measured, photoelectrons per digital unit was obtained.

By this method, at 18 kV accelerating voltage, the calibration of 1.18 photoelectrons/digital unit was established.

To determine the calibration at 18 kV a comparison was made of the same UV spot under both 15 kV and 18 kV acceleration. The results, in digital units, over a 10-pixel array is shown in the following table:

<u>Column</u>	<u>Digital Units*</u>				
	<u>59</u>	<u>60</u>	<u>61</u>	<u>62</u>	<u>63</u>
line 16	9, (2)	86, (13)	99, (35)	42, (16)	2, (0)
line 17	5, (4)	42, (9)	77, (25)	18, (9)	5, (3)

* In parenthesis 15 kV
 No parenthesis 18 kV

The central six pixels only were used here because the low level signals on the outer pixels can have high fractional errors due to digitization resolution and leakage current variations.

Since the electrons/second are identical for the two voltages, we can calculate for each pixel the electrons/digital unit at 15 keV by equating the electrons arriving per unit time in each case.

Using six central pixels, the mean value, calculated by weighting each value by the inverse of its variance, was calculated to be 3.61 photoelectrons/digital unit at 15 kV.

2.2.3 Electron Beam Spot Contour

The photoelectron spot pattern on the CCD is a convolution of the effects of the aberrations of the UV micro-projector lens, any focus errors in that lens, and in the Digicon magnetic lens.

Since, in general, the system was moved and refocused for each damage run, the spot contour was not constant. For each run the spot contour diagram was included with the data for that run (see Figures 9, 15 and 23).

The most extensive spot diagram, taken from the 18 kV (20°C) data, is shown in Figure 7. It is superimposed on the array pattern of the CCD202. This consists of columns of photosites 30 μm high by 18 μm wide with a 22 μm non-sensitive region between the columns. This non-sensitive region contains the readout shift registers and is covered by a layer of protective aluminum.

In taking the data of Figure 7, the photoelectron signal was typically very small compared to the leakage current. In addition, the leakage current changed (damage occurs) while the electron responsivity was being recorded; the array of Figure 8 is the leakage current pattern, corresponding to Figure 7, in computer digital units. Since this pattern is superimposed on the electron responsivity data, the leakage alone is taken before and after the responsivity data and its mean value subtracted to obtain the electron signal.

In the spot contour of Figure 7, three values are given for each pixel; topmost is the digital units remaining

		COLUMN				
		65	66	67	68	69
LINE	15	0 0 0	2 2.4 20	2 2.4 20	2 2.4 20	2 2.4 20
	16	3 3.5 29	6 7.1 59	5 5.9 49	3 3.5 29	3 3.5 29
	17	4 4.7 39	13 15 130	9 11 88	4 4.7 39	5 5.9 49
	18	18 21 180	61 72 600	49 58 480	20 24 200	1 1.2 9.8
	19	35 41 340	132 156 1290	67 79 660	16 19 160	5 5.9 49
	20	29 34 280	92 110 900	48 57 470	10 12 98	1 1.2 9.8
	21	10 12 98	34 40 330	15 18 150	4 4.7 39	2 2.4 20
	22	9 11 88	6 7.1 59	3 3.5 29	3 3.5 29	3 3.5 29
	23	2 2.4 20	3 3.5 29	2 2.4 20	1 1.2 9.8	-2 0 0

— digital units/10 frames
 — electrons/10 frames
 — electrons/second

Figure 7. Electron Beam Spot Contour
18 keV, 25°C

	COLUMN				
	65	66	67	68	69
15	210	196	195	195	173
16	213	207	180	160	180
17	207	212	193	190	174
18	181	196	166	164	181
19	195	210	198	197	163
20	190	197	181	189	168
21	191	189	194	190	194
22	170	178	178	183	168
23	180	189	189	182	190

Figure 8. Leakage Current (in digital units/10 frames)
at Electron Beam Location 18 keV, 25°C

from the leakage current subtraction (10 summed frames); middle is the electron flux in electrons/10 frames/pixel obtained by the calibration of 1.18 photoelectrons/digital unit; bottom is the electron flux in electrons/sec-pixel.

2.3 Electron Beam Damage

Using the system and techniques just described, damage phenomena were observed under three basic conditions:

1. 15 keV electrons; 25°C temperature
2. 18 keV electrons; 25°C temperature
3. 18 keV electrons; 0°C temperature

Under these conditions, five effects were recorded for analysis:

1. change in leakage current as a function of electron dose
2. change in photoelectron responsivity as a function of electron dose
3. change in visible light responsivity as a function of electron dose
4. damage effects in pixels not in the electron beam spot (collateral damage)
5. effects of variation in clock voltage

It appears that three components are present in the damage phenomena:

1. damage which is dependent on the dose
2. damage which depends on events in adjacent or nearby pixels (collateral damage)
3. damage which seems peculiar to that pixel, or cannot otherwise be explained

In addition, damage which is a function of the flux was looked for, but was not seen. Early suggestions of such an effect were apparently due to a problem in observational selection.

Five damage runs were conducted:

1. 18 keV electron energy. This test yielded preliminary leakage current data. Responsivity data were not valid due to faulty experimental procedures. Other phenomena were not observed.
2. 15 keV electron energy. This test was aborted due to faulty data acquisition system. No valid data were obtained.
3. 15 keV electron energy, 25°C array temperature. This repeat of the preceding test was successful. Valid leakage and responsivity data were obtained and the effect of variation in the lower level of the photogate clock voltage, ϕ_{PL} were observed.
4. 18 keV electron energy, 25°C array temperature. This test was successful. Valid leakage and responsivity data were obtained. Collateral damage in adjacent and nearby pixels was observed as was the effect of variations in the ϕ_{PL} clock voltage.
5. 18 keV electron energy, 0°C array temperature. This test was successful. Valid leakage and responsivity data were obtained.

Results from the latter three tests are included here. The data are presented either as a function of electron dose or

of time. The graph ordinate scales are percent of saturation of the array as determined with visible (tungsten filament) light.

2.3.1 15 keV; 25°C

The results of the 15 keV damage are presented in Figures 9 through 14. The test was performed with the CCD array at room temperature and the total duration of the test was 76 minutes.

The beam spot contour (Figure 9) is shown in the same format as was done for the beam contour discussion in Section 2.2.3. Data from the central six pixels (lines 16 and 17, columns 60 through 62) are shown on the subsequent graphs.

Figure 10 is a plot of the increase in leakage current as a function of total electron dose per pixel. Each curve is identified by the line and column of the corresponding pixel. The curve of 17-62 is coincident with that of 17-60. All curves show the same general shape—an initial drop followed by a linear rise to a peak, followed by a decline as the pixel ceases to function. The initial drop in leakage appears to be a real physical phenomenon and not caused by experimental procedures, as it is dose related rather than occurring simultaneously for all pixels. The damage peak was reached for the two pixels having the highest flux and occurred at a dose of 2 to 3×10^6 electrons.

The slight change in slope on a given curve for some of the leakage current curves (example 16-60) may be a physical or an experimental phenomenon, but a physical cause

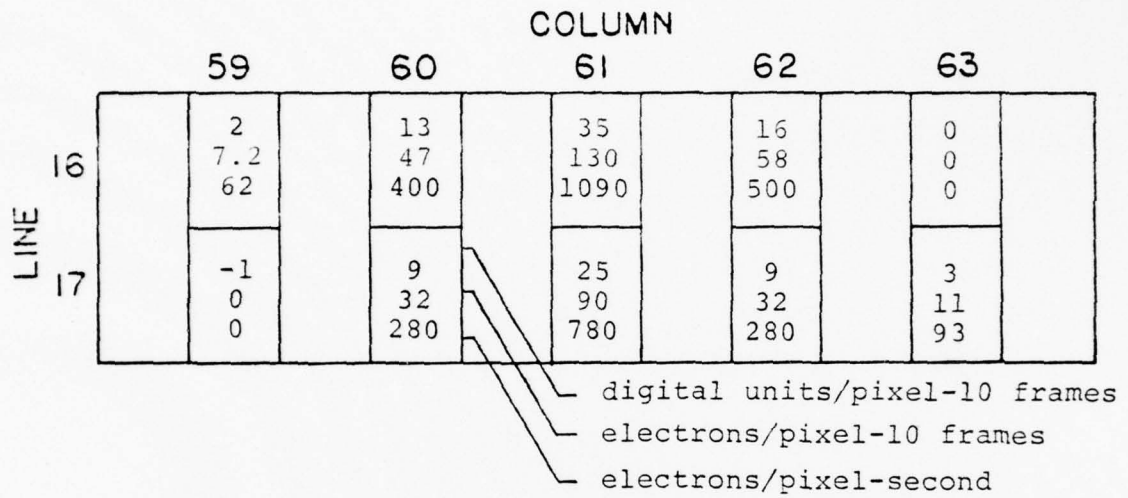


Figure 9. 15 kV Spot Contour

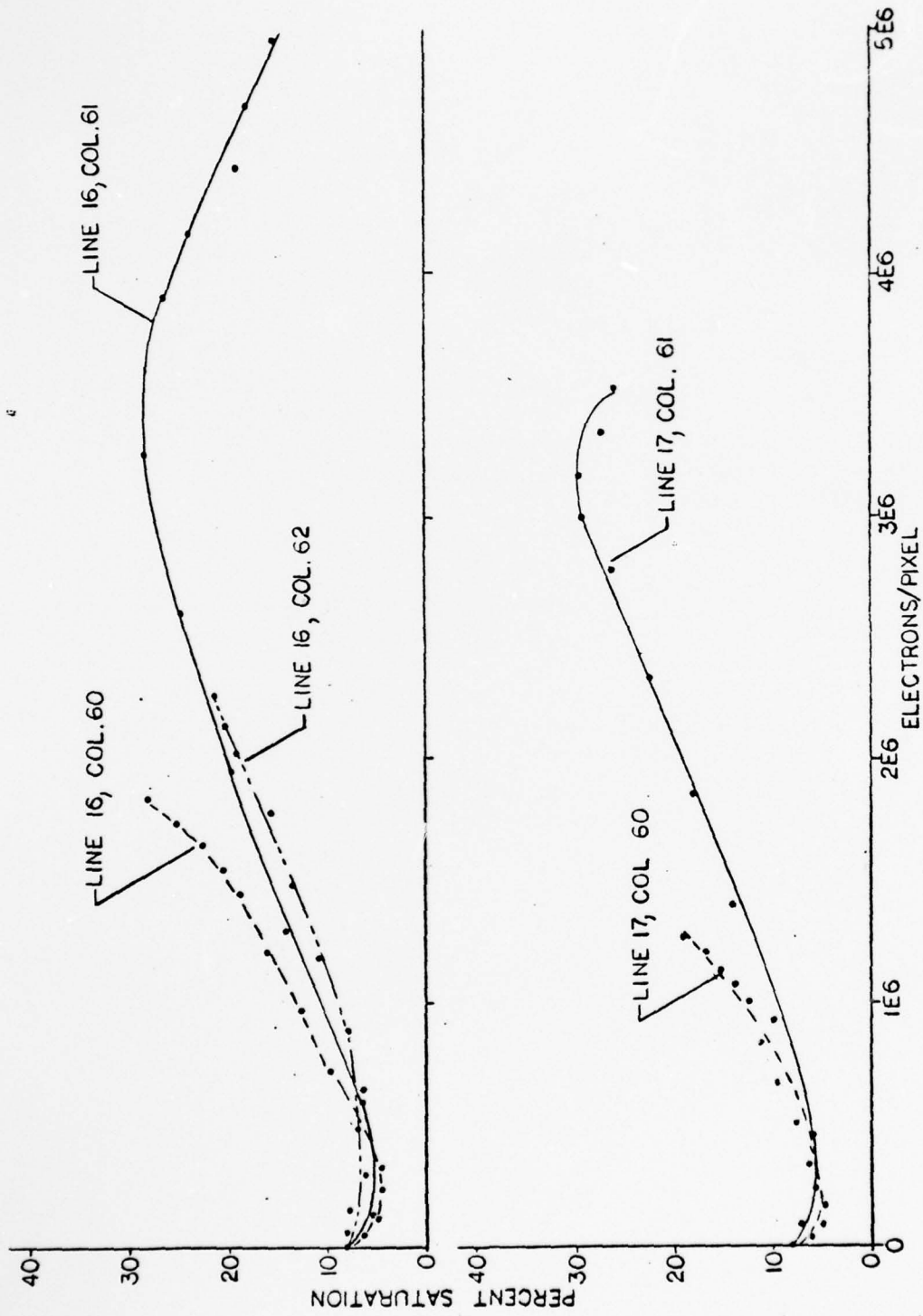


Figure 10. LEAKAGE CURRENT AS A FUNCTION OF FLUENCE;
15 keV, 25 C

is suggested because it occurred in only some pixels and not simultaneously in time for all pixels.

The curves of Figure 11 show the photoelectron beam signal as a function of dose. The scatter in the data reflects the difficulty in making the measurement. Very small changes in the electron beam position or intensity can make large variations in the measured signal. In particular, many of the variations near the end of the test period occurred simultaneously and so are considered to be an experimental system effect. Nevertheless, the trend is toward lower responsivity at high doses.

Figure 12 shows the response of the two highest flux pixels to the visible light tungsten lamp. The variation near the end of the irradiation are real; all other pixels showed constant output during the entire time period. The final recovery of 16-61 is also real. See the data taken at 18 keV, 0°C (Section 2.3.3) for more examples of this type of effect.

At the completion of the test, the leakage current and relative electron and visible light responsivity were measured for various values of the lower level of the photogate clock voltage, ϕ_{pL} . This is the clock voltage which was found during previous experiments to have the greatest effect on the "field splitting" of the leakage current. In this effect the leakage in one of the interlaced fields becomes systematically higher or lower than that of the other field, and it was found empirically that this effect was sensitive to the ϕ_{pL} clock voltage.

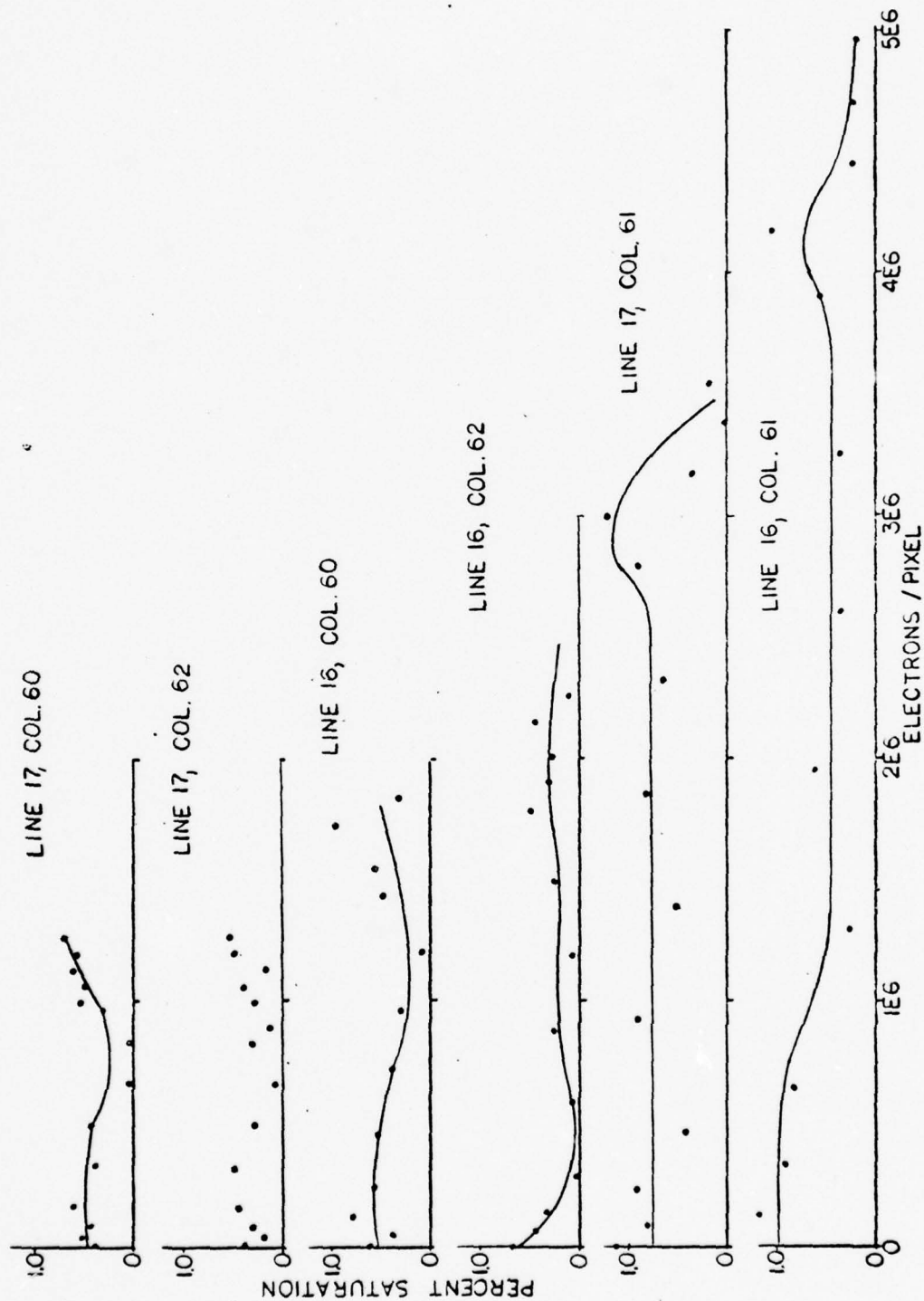


Figure 11. PHOTOELECTRON BEAM SIGNAL AS A FUNCTION OF FLUENCE;
15 keV, 25°C

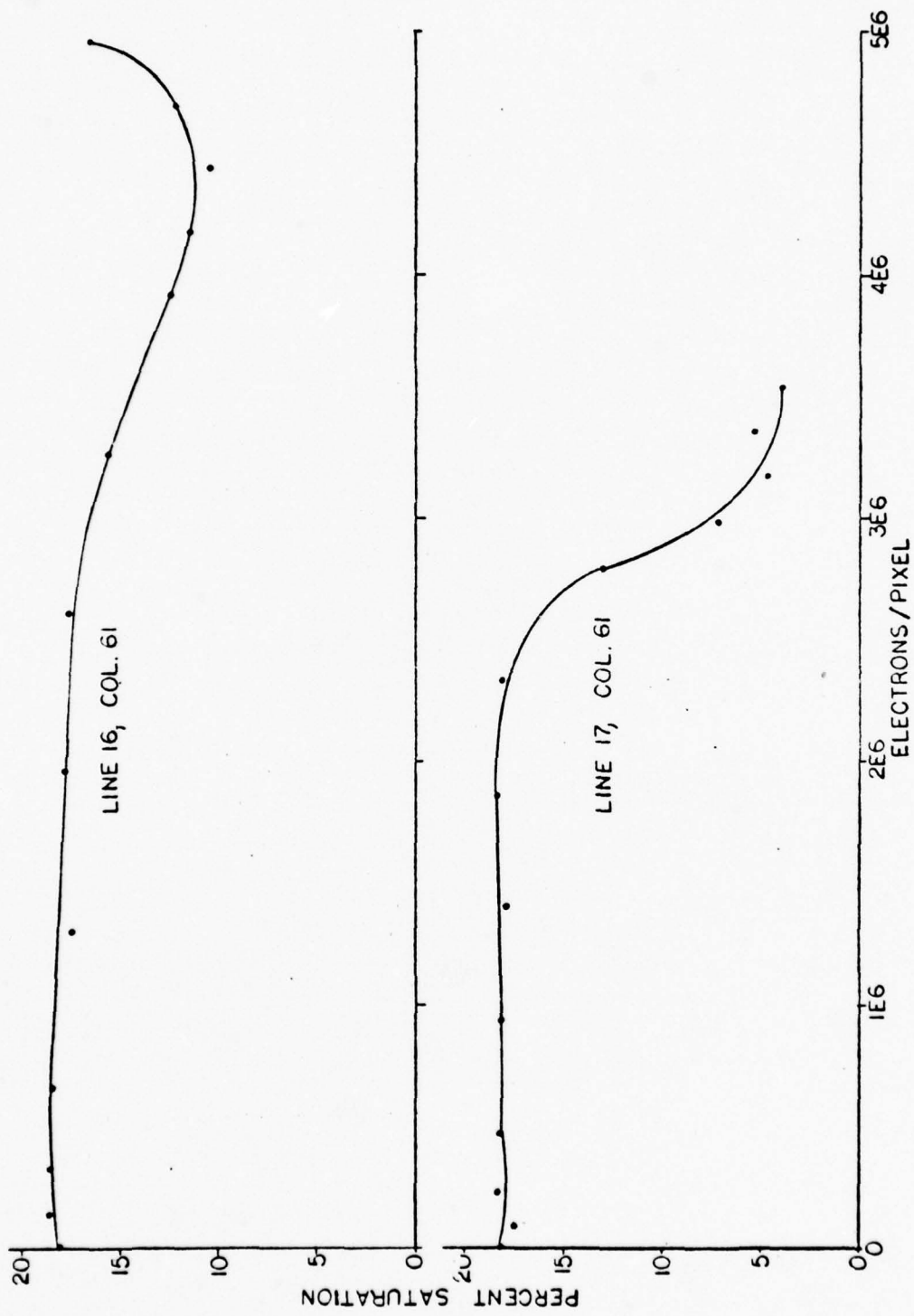


Figure 12. RESPONSE TO VISIBLE LIGHT AS A FUNCTION OF FLUENCE;
15 keV, 25°C

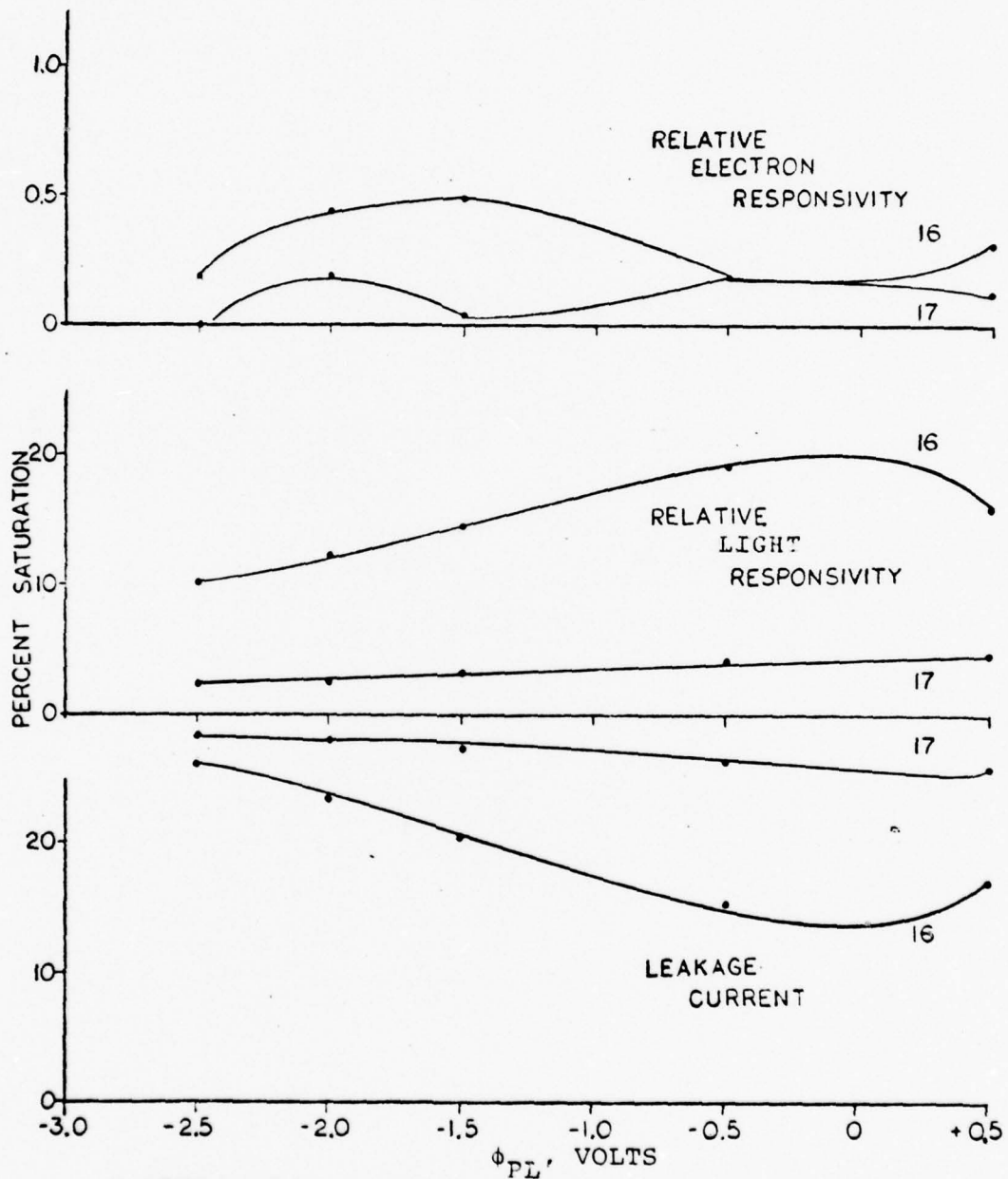
Prior to this damage test, the clock voltages were set to those values which were judged to give the best array performance. The optimum value for ϕ_{PL} was -0.5 volts.

The results of varying ϕ_{PL} at the conclusion of the test are shown for lines 16 and 17, column 61, in Figure 13. The leakage currents in the two fields become more nearly the same as the voltage is decreased to more highly negative values. The optimum value is thus a function of dose and would probably have to be adjusted periodically for best performance. No similar data were taken on this pair of pixels at other doses, but Figure 14 shows the same phenomena for the two fields in columns 60, 61, and 62 which at this time had a different dose. No change in the optimum ϕ_{PL} is apparent at any dose except the high dose of columns 61.

2.3.2 18 keV; 25°C

A similar test of electron beam damage was performed with 18 keV photoelectrons. Data were taken over a larger number of pixels so that the effects on the parameters away from the immediate spot location could be evaluated (these data are discussed in Section 2.3.4, Collateral Damage).

The electron beam contour, Figure 15, is the same as was used for the spot contour discussion of Section 2.2.3. The leakage current (Figure 16, 17, 18), the photoelectron signal (Figures 19, 20) and the visible light signal (Figures 21, 22) are presented in the same format as was used for the 15 keV data (although the graph scales are different).



NOTE: LINE 16 (A FIELD), COL. 61
 LINE 17 (B FIELD), COL. 61

Figure 13. EFFECT OF ϕ_{PL} ON TEST PARAMETERS

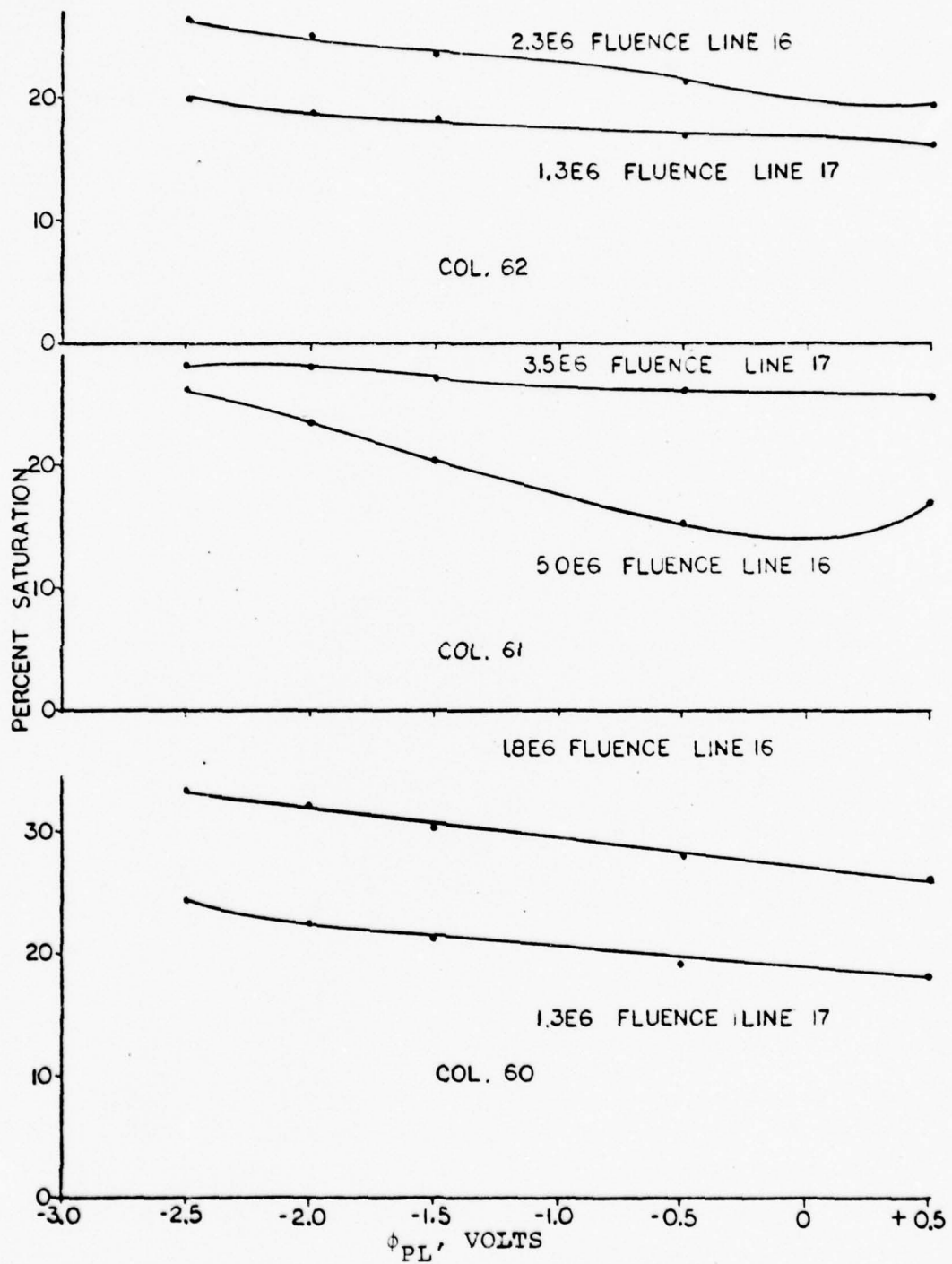


Figure 14. EFFECT OF ϕ_{PL} ON CCD DARK CURRENT

The data appear more erratic than the 15 keV data. This tendency increased in the 18 keV, 0°C data (Section 2.3.3).

As in the case of 15 keV, the pixels for which the leakage current increased cease to be responsive to photoelectrons at about 10^6 electrons fluence. The reason for the decreasing leakage current in column 67 is not known; both fields (odd and even line numbers) were affected in the same manner.

2.3.3 18 keV; 0°C

A second set of damage data was obtained at 18 keV electron energy with the rear plate of the Digicon tube maintained at a temperature of 0°C. Thermal contact to the CCD array was by means of a copper block clamped against the back of the CCD array DIP package and soldered to the inside of the Digicon rear plate. Cold dry nitrogen was blown against the rear plate to preclude condensation and the plate temperature was monitored with a thermistor.

The array was exposed to the electron flux for a period of 59 minutes, with data taken at 2 minute intervals. The pixels exhibited peculiar individual behavior with respect to leakage current, electron responsivity, and visual light responsivity. These are shown on the following set of graphs, Figures 23 through 28.

Figure 23 is the electron beam spot contour. The flux at the peak is 1500 electrons/pixel-second, or approxi-

		COLUMN				
		65	66	67	68	69
LINE	15	0 0 0	2 2.4 20	2 2.4 20	2 2.4 20	2 2.4 20
	16	3 3.5 29	6 7.1 59	5 5.9 49	3 3.5 29	3 3.5 29
	17	4 4.7 39	13 15 130	9 11 88	4 4.7 39	5 5.9 49
	18	18 21 180	61 72 600	49 58 480	20 24 200	1 1.2 9.8
	19	35 41 340	132 156 1290	67 79 660	16 19 160	5 5.9 49
	20	29 34 280	92 110 900	48 57 470	10 12 98	1 1.2 9.8
	21	10 12 98	34 40 330	15 18 150	4 4.7 39	2 2.4 20
	22	9 11 88	6 7.1 59	3 3.5 29	3 3.5 29	3 3.5 29
	23	2 2.4 20	3 3.5 29	2 2.4 20	1 1.2 9.8	-2 0 0

— digital units/10 frames
 — electrons/10 frames
 — electrons/second

Figure 15. PHOTOELECTRON BEAM SPOT
CONTOUR 18keV, 25°C

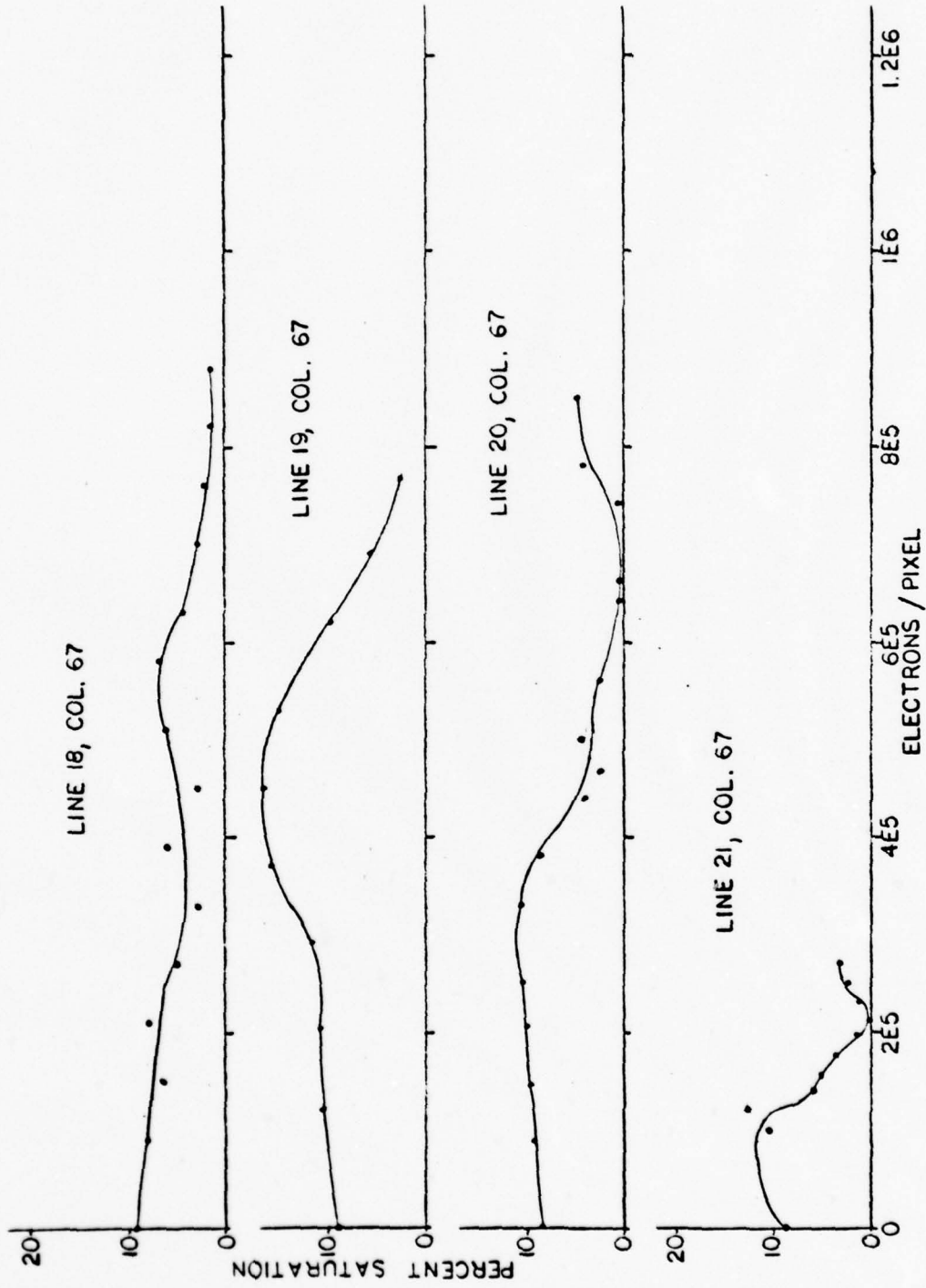


Figure 16. LEAKAGE CURRENT AS A FUNCTION OF FLUENCE;
18 keV, 25°C

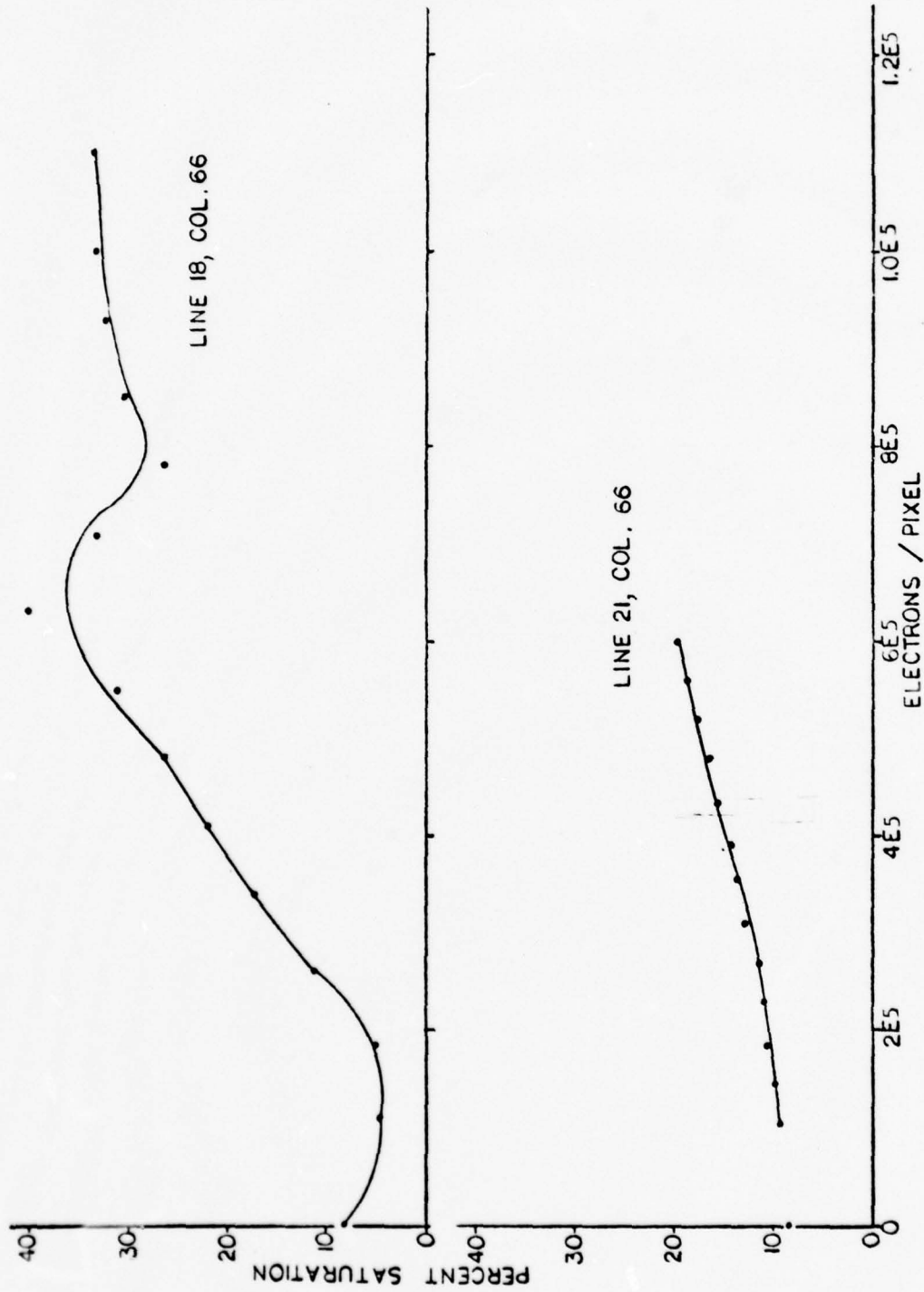


Figure 17. LEAKAGE CURRENT AS A FUNCTION OF FLUENCE;
18 keV, 25°C

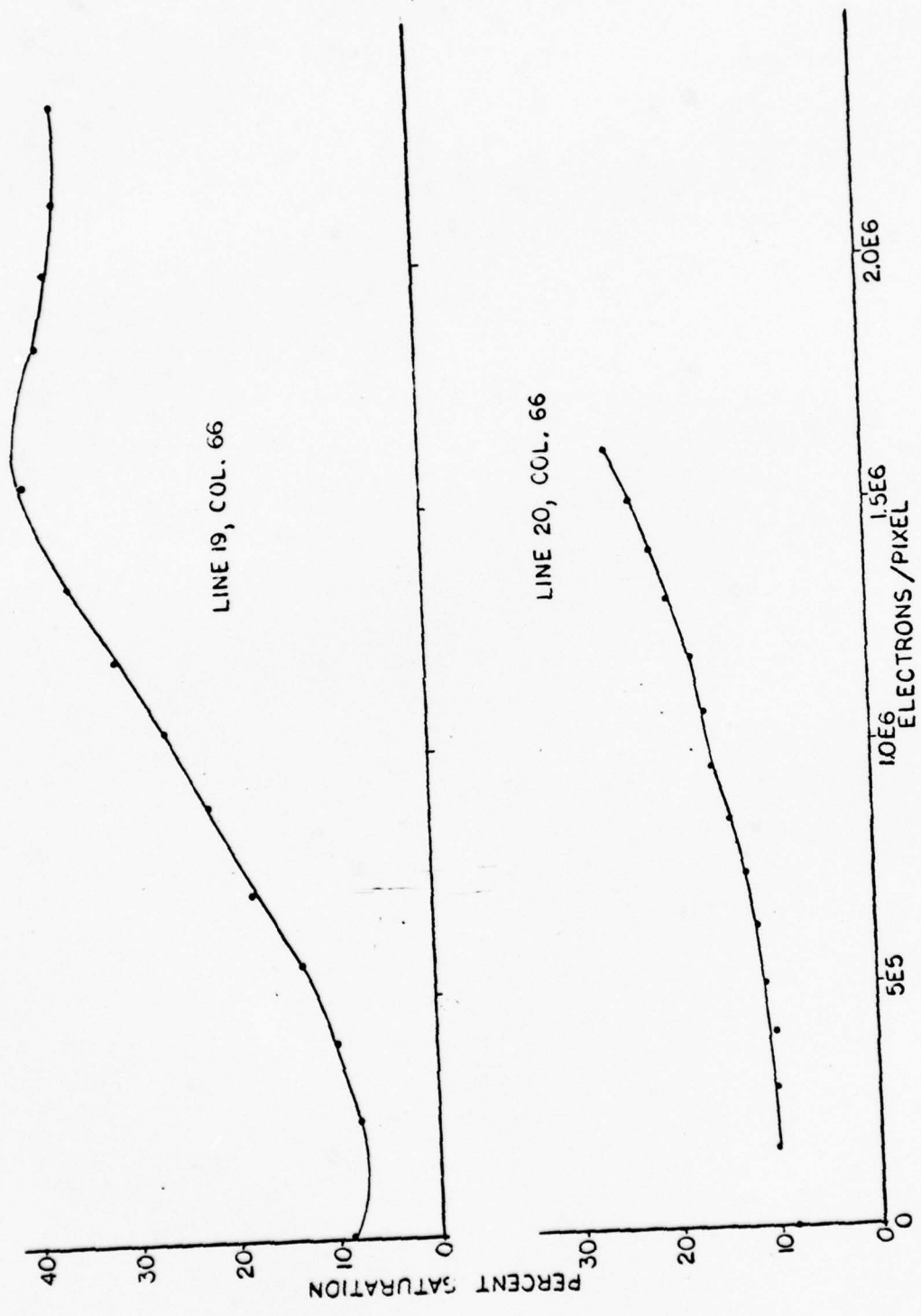


Figure 18. LEAKAGE CURRENT AS A FUNCTION OF FLUENCE;
18 keV, 25°C

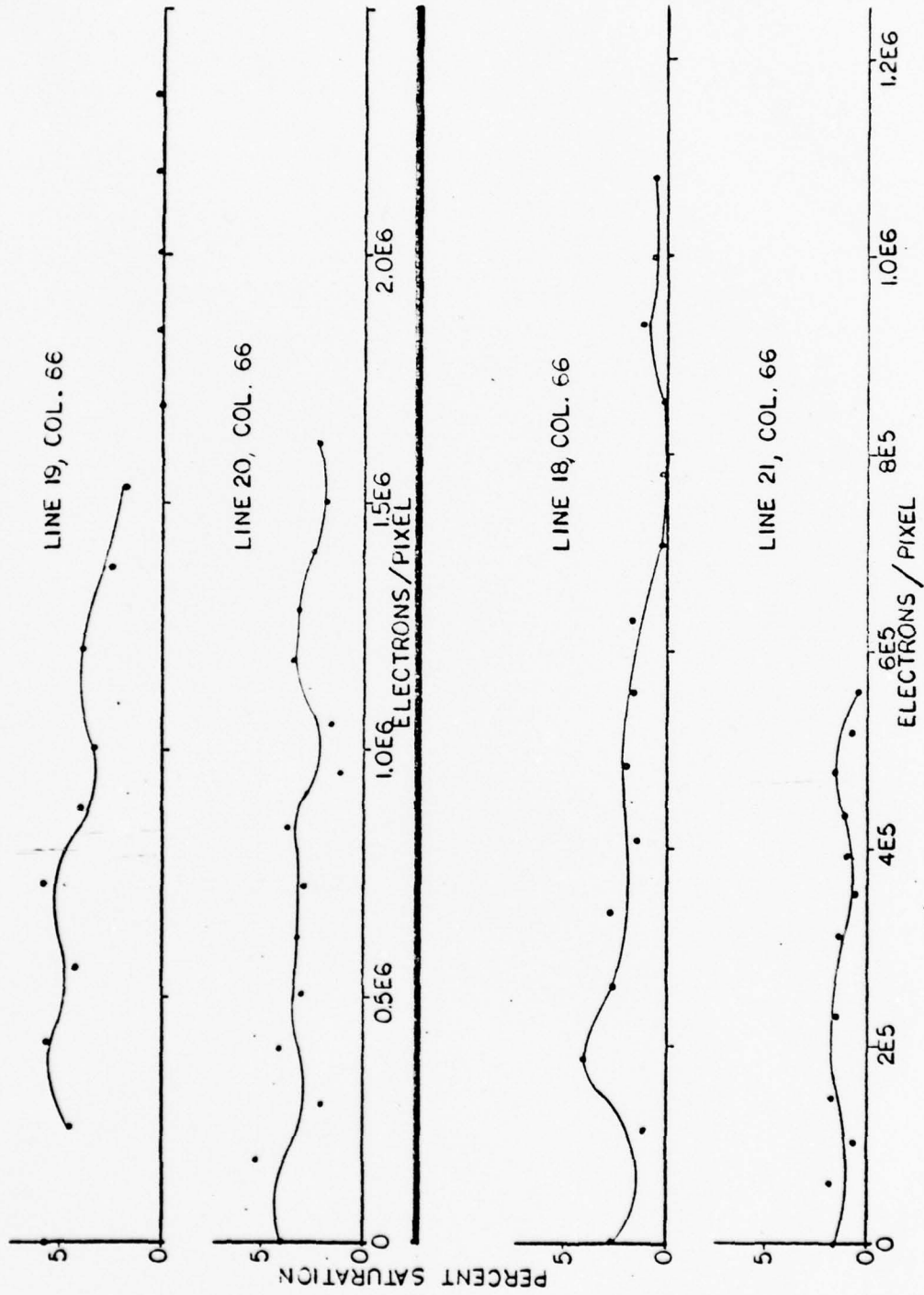


Figure 19. PHOTOELECTRON BEAM SIGNAL, AS A FUNCTION OF FLUENCE;
18 keV, 25°C

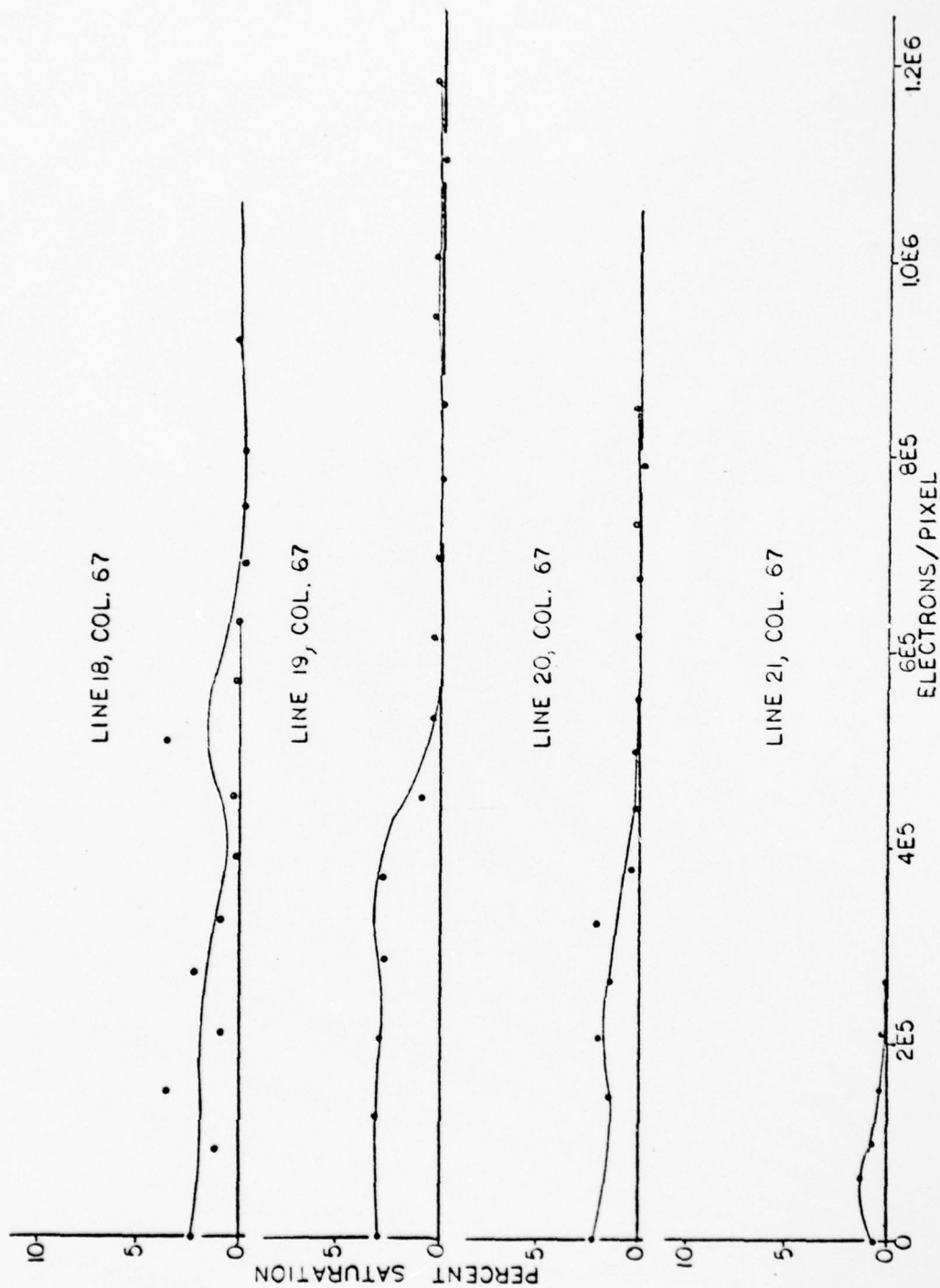


Figure 20. PHOTOELECTRON BEAM SIGNAL AS A FUNCTION OF FLUENCE;
18 keV, 25°C

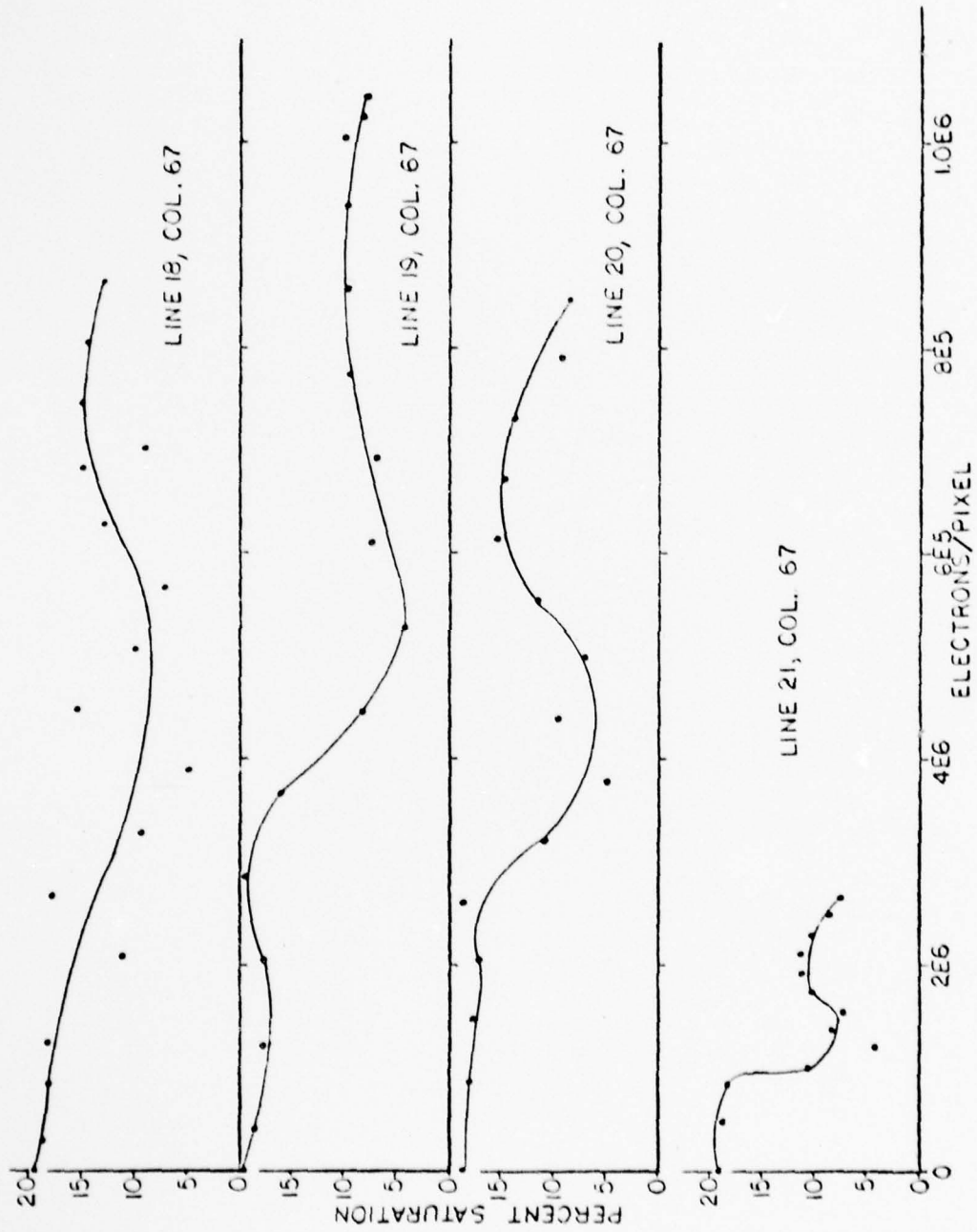


Figure 21. RESPONSE TO VISIBLE LIGHT AS A FUNCTION OF FLUENCE;
18 keV, 25°C

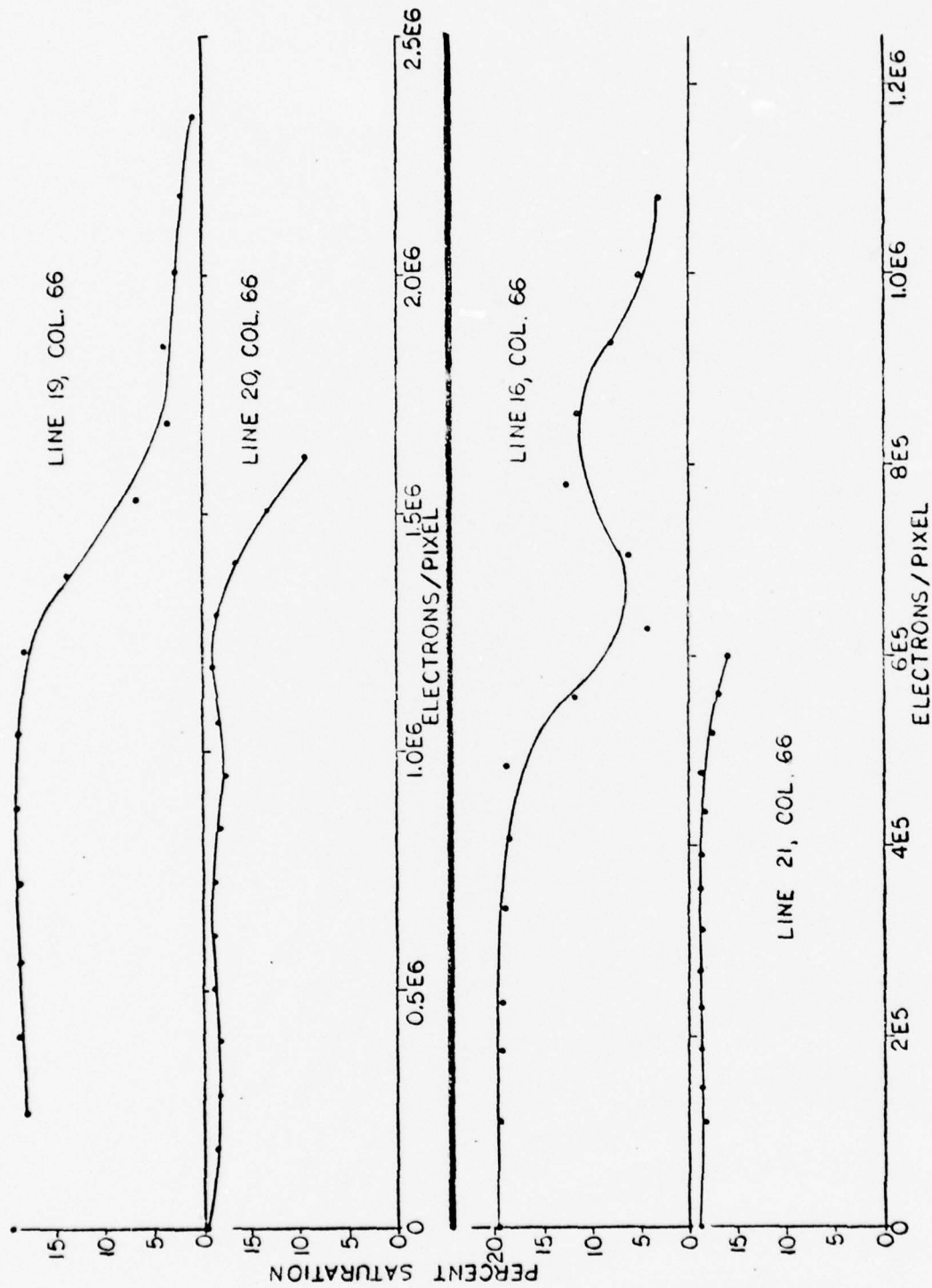


Figure 22. RESPONSE TO VISIBLE LIGHT AS A FUNCTION OF FLUENCE;
18 keV, 25°C

mately 17.6 electrons/pixel-frame.

Figure 24, 25 and 26 are, respectively, the leakage current, photoelectron signal, and visible light signal plotted as a function of electron fluence per pixel. The six panels are presented in the same order on the three figures with the pixel receiving the lowest electron beam flux at the top and with the increasing fluxes on successively lower graphs.

The leakage current before damage, and the rate of electron damage, are reduced at this reduced temperature as expected. Pixel lifetime is not correspondingly increased, however. The response to photoelectrons ceased at fluences of about 10^6 electrons. Individual pixel behavior varied considerably and this variance was much more pronounced than at higher temperatures.

To demonstrate the reality of these effects, Figure 27 shows the visual light signal from sequential pixels across one line passing through the electron spot as a function of time. The constancy of the light source with time is shown by the steady response of the pixels on either side of the electron spot; the bizarre behavior of the pixels in the spot is thus considered to be real.

In a like manner, Figure 28 is a plot of the photoelectron signal as a function of time for the six panels in the spot center. The lack of correlation among the curves indicates that the UV lamp intensity did not change abruptly.

LINE	COLUMN						
	69	70	71	72	73	74	75
56	0 0 0	0 0 0	7 8.3 71	4 4.7 41	6 7.1 61	4 4.7 41	6 7.1 61
57	0 0 0	1 1.2 10	7 8.3 71	50 59 510	19 22 190	10 12 100	0 0 0
58	0 0 0	0 0 0	36 43 366	128 150 1300	46 54 470	5 5.9 51	0 0 0
59	0 0 0	9 11 91	45 53 457	149 180 1500	92 110 930	2 2.4 20	0 0 0

— digital units/10 frames
 — electrons/10 frames
 — electrons/second

Figure 23. Electron Beam Spot Contour
18 keV, 0°C

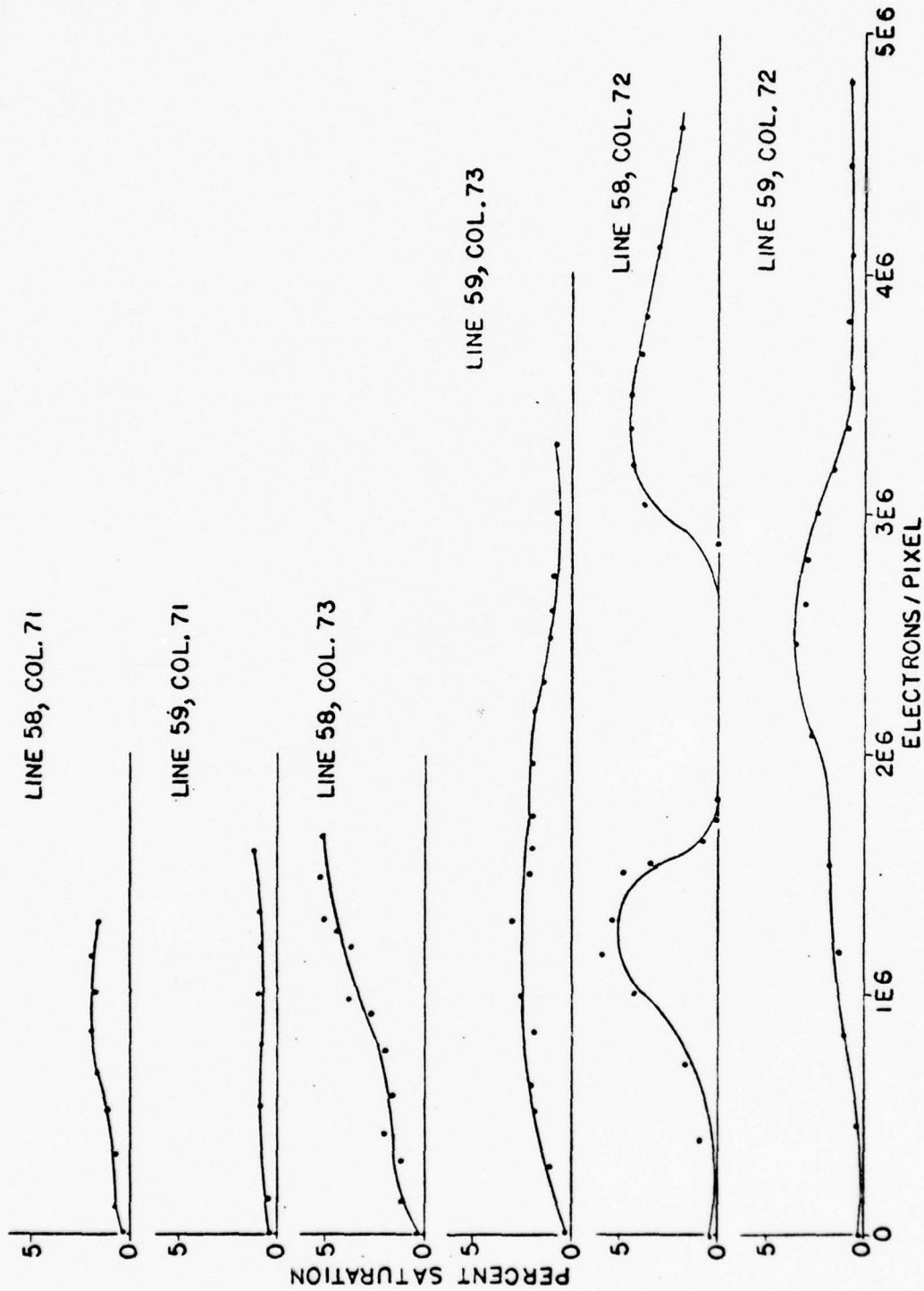


Figure 24. LEAKAGE CURRENT AS A FUNCTION OF FLUENCE;
18 keV, 0°C

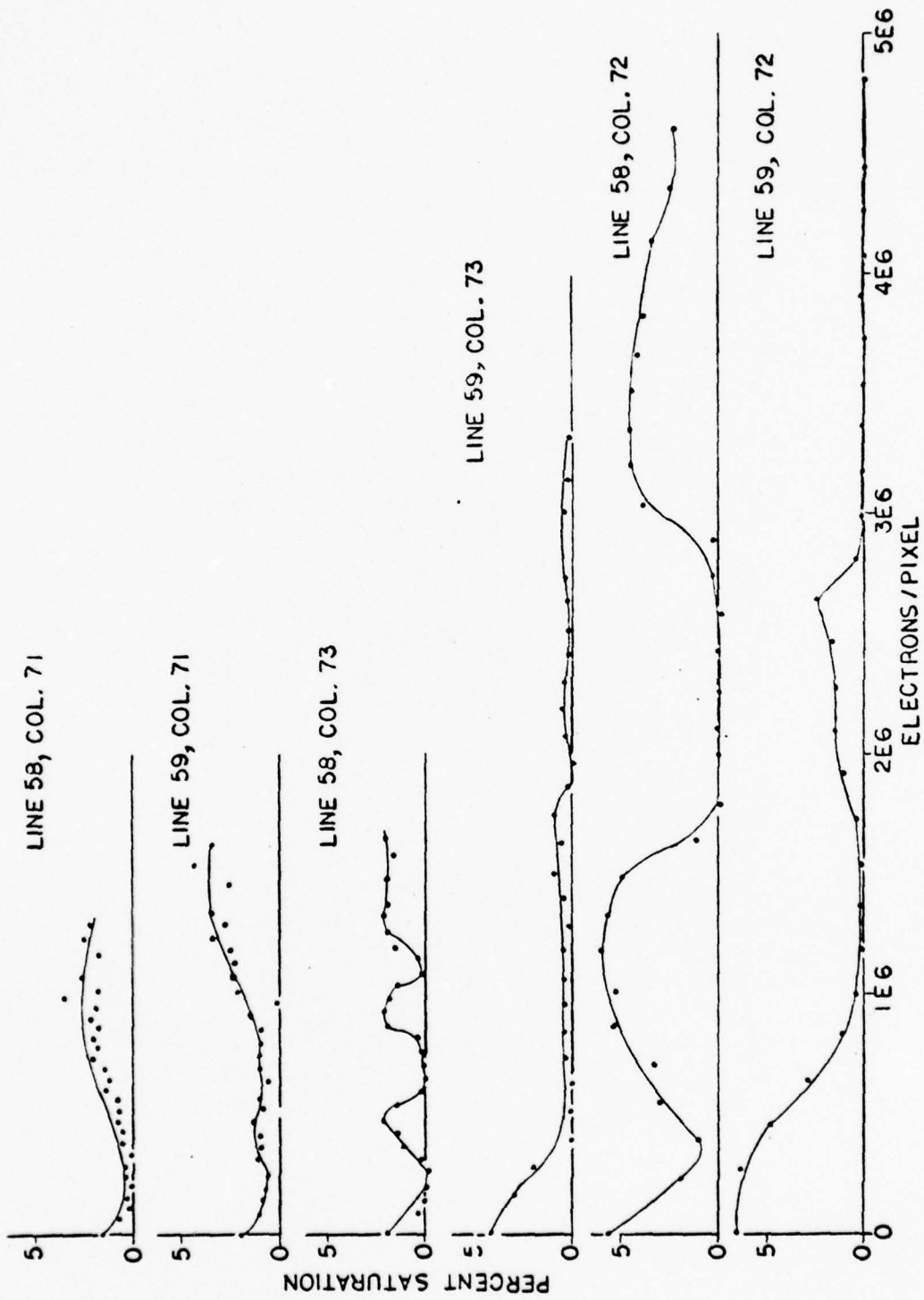


Figure 25. PHOTOELECTRON BEAM SIGNAL AS A FUNCTION OF FLUENCE;
18 keV, 0°C

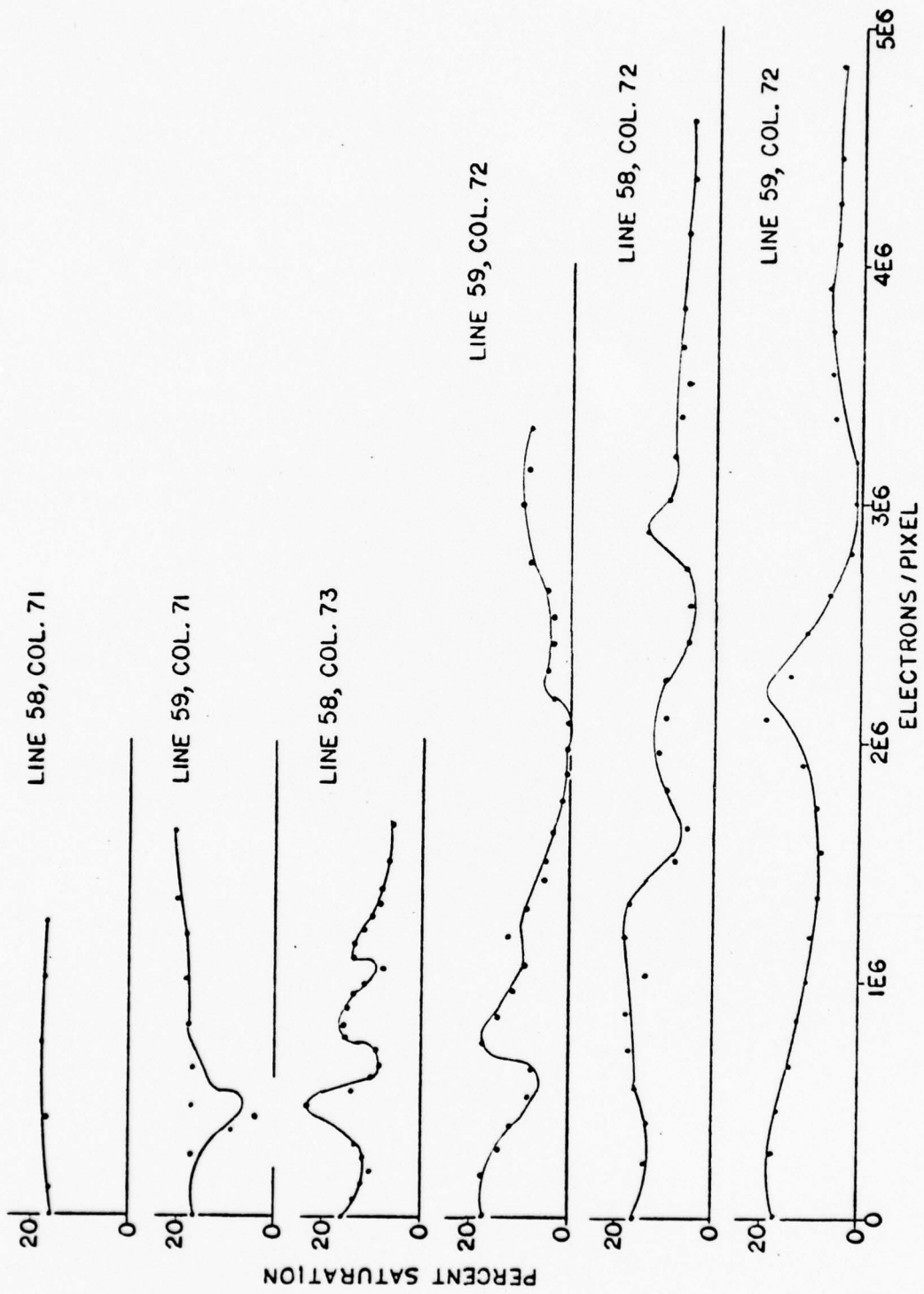


Figure 26. RESPONSE TO VISIBLE LIGHT AS A FUNCTION OF FLUENCE;
18 keV, 0°C

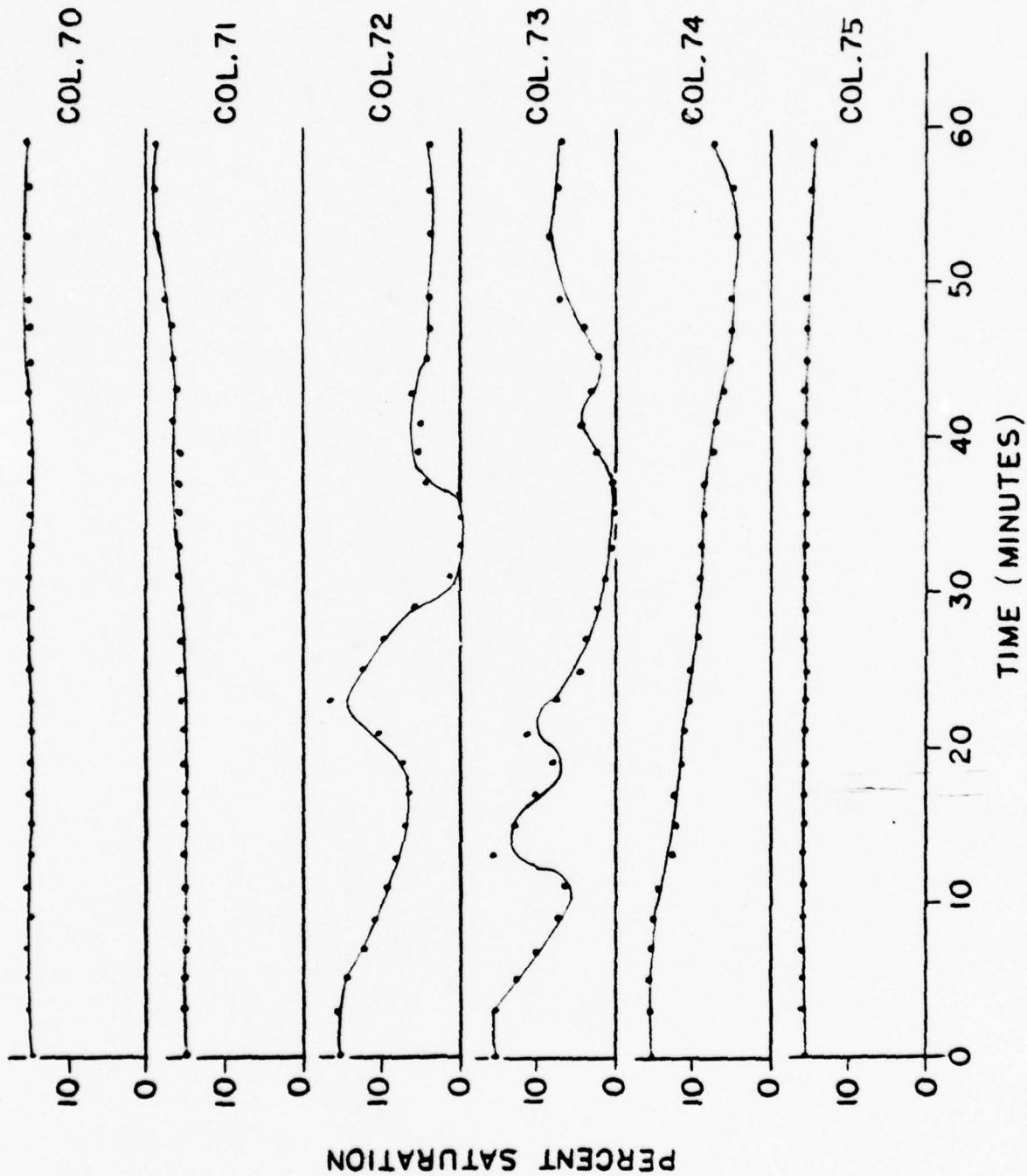


Figure 27. RESPONSE TO VISIBLE LIGHT ACROSS ELECTRON SPOT, LINE 59;
18 keV, 0°C

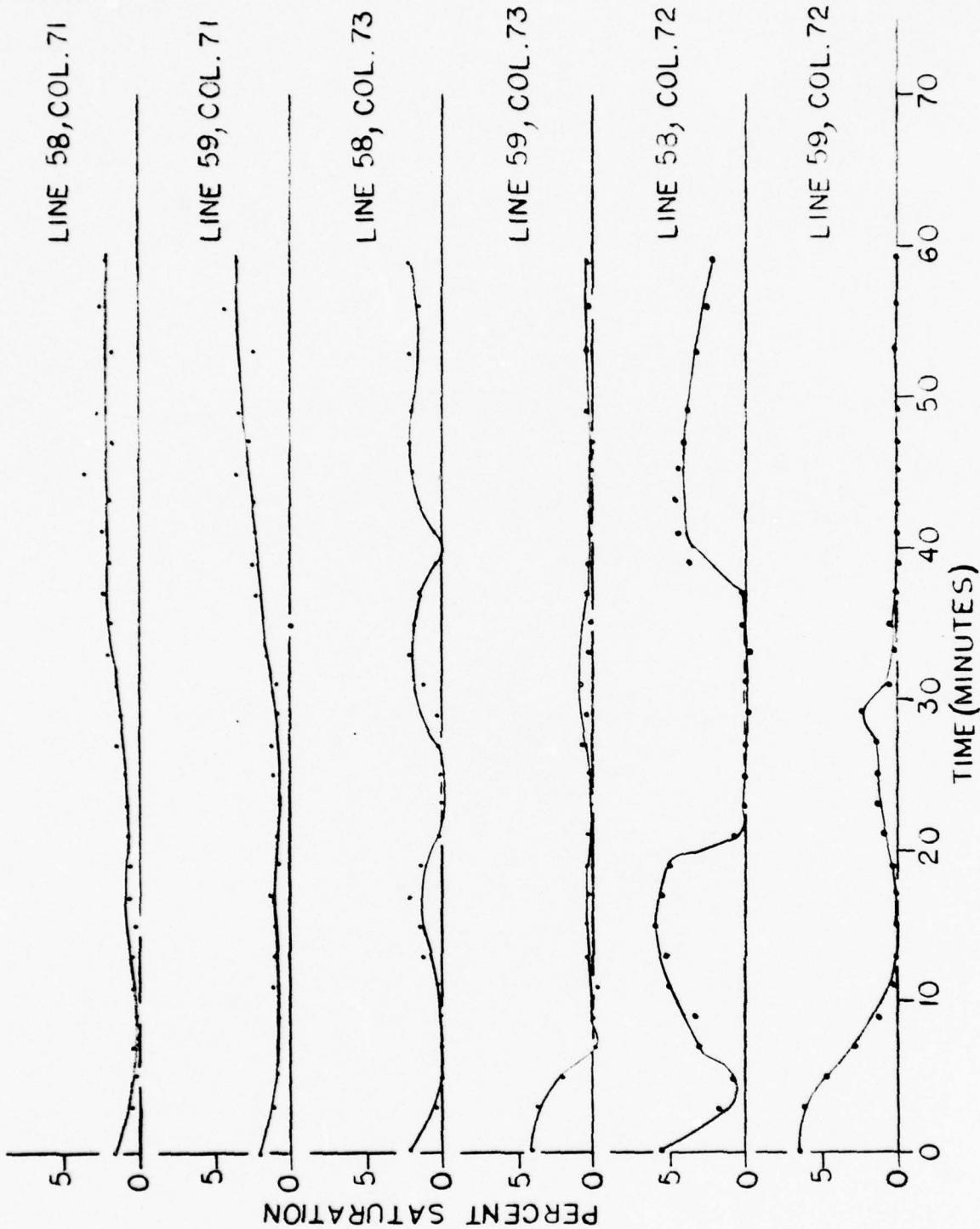


Figure 28. PHOTOELECTRON BEAM SIGNAL ACROSS ELECTRON SPOT;
18 keV, 0°C

The electron spot may have moved on the array, but the apparent reality of the variations in visible light responsivity implies that these electron responsivity curves also reflect actual changes occurring in the CCD array.

2.3.4 Collateral Damage

Visual monitoring of the leakage current damage pattern during the electron bombardment showed that damage occurs first in the vicinity of the electron spot, then spreads vertically. To study this phenomenon an array of pixels 5 columns wide and 20 columns high was recorded during the 18 kV (25°C) test run.

For convenience the 18 kV spot diagram is repeated in Figure 29. The peak flux of 1290 electrons/pixel-second is on line 19, column 66.

On a monitor oscilloscope showing visually the leakage current pattern, the leakage is seen to increase over the entire column containing the damage spot. If this was caused by damage to the column shift register in the location of the spot, it would affect the data from the "upstream" pixels which must pass through the damage but should not affect the data from pixels "downstream" in the register. The leakage increase was seen to spread in both directions from the damage spot, indicating that the damage was not occurring in this shift register.

		COLUMN				
		65	66	67	68	69
15	0	2	2	2	2	2
	0	2.4	2.4	2.4	2.4	2.4
16	0	20	20	20	20	20
	3	6	5	3	3	
17	3.5	7.1	5.9	3.5	3.5	
	29	59	49	29	29	
18	4	13	9	4	5	
	4.7	15	11	4.7	5.9	
19	39	130	88	39	49	
	18	61	49	20	1	
20	21	72	58	24	1.2	
	180	600	480	200	9.8	
21	35	132	67	16	5	
	41	156	79	19	5.9	
22	340	1290	660	160	49	
	29	92	48	10	1	
23	34	110	57	12	1.2	
	280	900	470	98	9.8	
24	10	34	15	4	2	
	12	40	18	4.7	2.4	
25	98	330	150	39	20	
	9	6	3	3	3	
26	11	7.1	3.5	3.5	3.5	
	88	59	29	29	29	
27	2	3	2	1	-2	
	2.4	3.5	2.4	1.2	0	
28	20	29	20	9.8	0	

— digital units/10 frames
 — electrons/10 frames
 — electrons/second

Figure 29. PHOTOELECTRON BEAM SPOT CONTOUR;
18 keV, 25°C

Figures 30 through 33 show the leakage current for each pixel down the column for columns 65 through 68, respectively. The four sets of data in each figure correspond to the time at which the dose on the highest flux pixel (line 19, column 66) was 4.0×10^5 , 1.0×10^6 , 1.7×10^6 , and 2.3×10^6 electrons. The leakage current increase in the damage spot is obvious; the increase above (in the column) and below the damage spot is small but real. Away from the spot center the leakage increased from typically 8% of saturation to 10% of saturation.

The large increase in leakage at line 16, column 67 (Figure 32) is anomalous in that it does not correspond to a region of high electron flux. To determine if the electron spot moved during the test, Figure 34 shows a sequence of the recorded photoelectron signals for each pixel in 3×10 array centered in the spot center. The spot is seen centered at line 19, column 66 at $t=0$ minutes and a very low flux is seen at line 16, column 67. Although the pixel at the center of the spot showed a lower signal as time progressed, this appears to be a loss of responsivity and the spot appears to remain centered at that location. At several times (e.g., $t=9$ min., line 17, column 67) a high electron signal is seen which does not correspond to the nominal spot contour. This appears to be anomalous pixel behavior since it is not clear how the electron flux could achieve the contour shown by the signal.

Figure 35 is the responsivity to visual light, determined, as in the bombardment damage data, by flooding the array with uniform illumination from a tungsten filament. The graph is the same format as Figure 31, showing the visual light

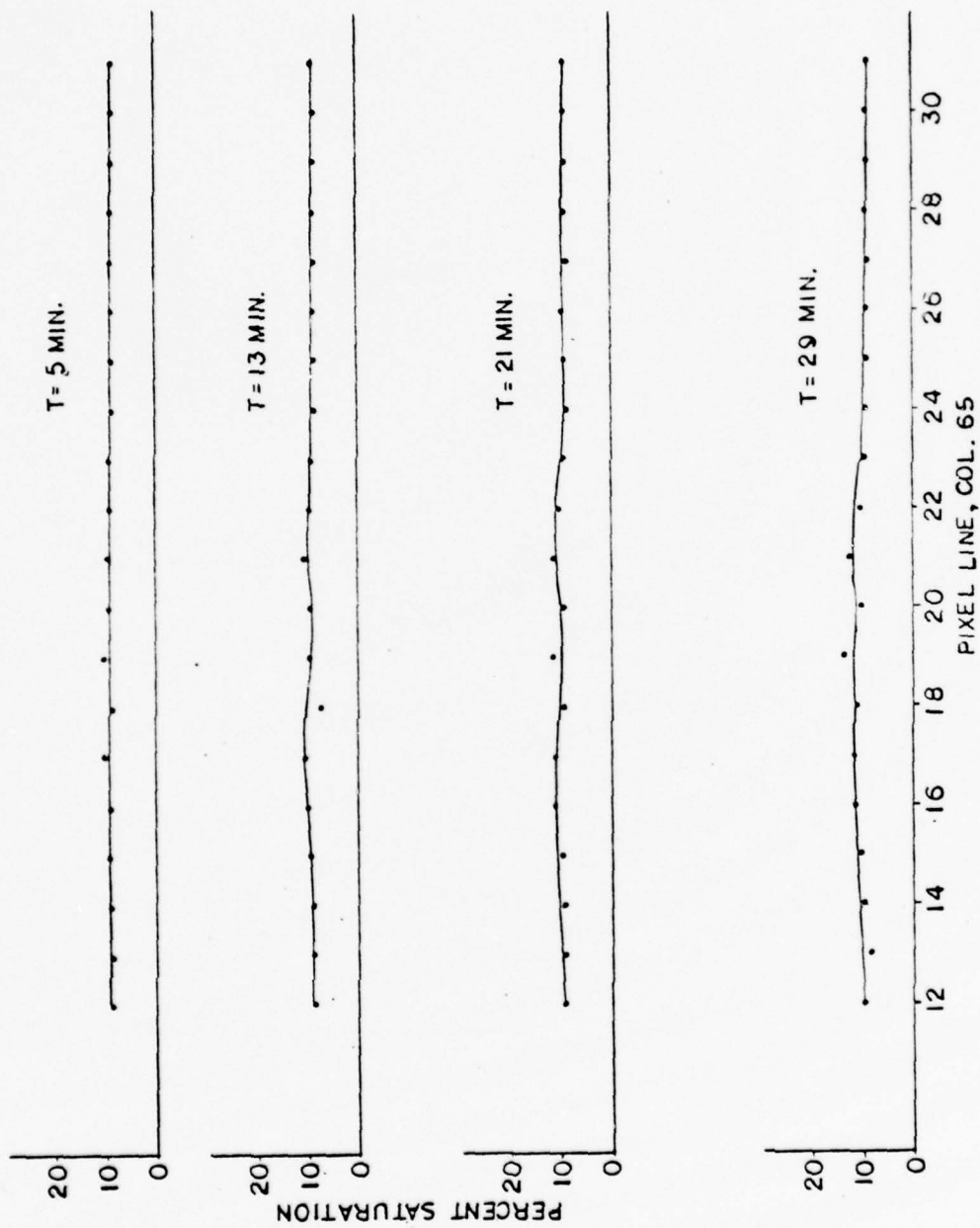


Figure 30. COLLATERAL DAMAGE: COLUMN 65 LEAKAGE CURRENT;
18 keV, 0°C

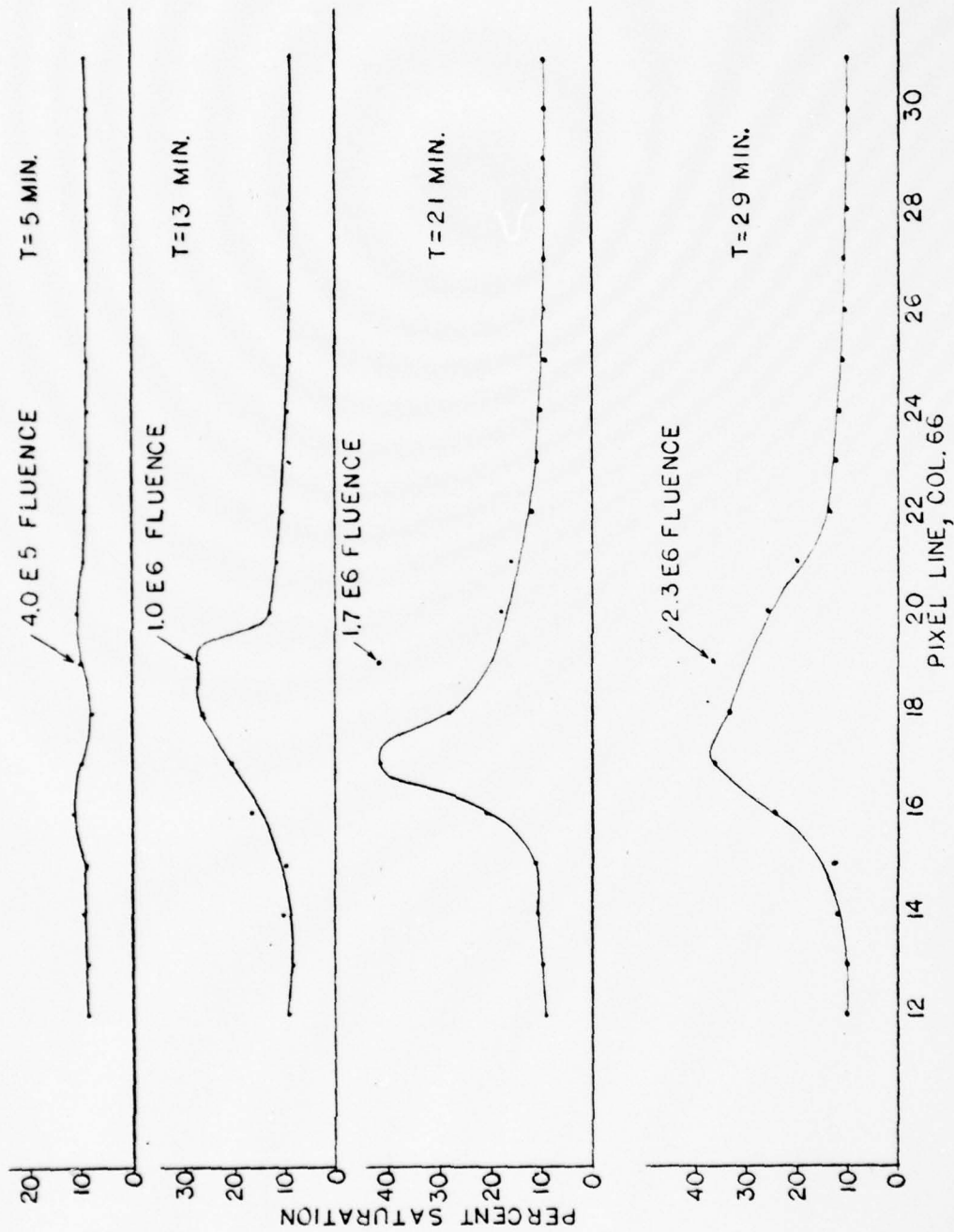


Figure 31. COLLATERAL DAMAGE: COLUMN 66 LEAKAGE CURRENT;
18 keV, 0°C

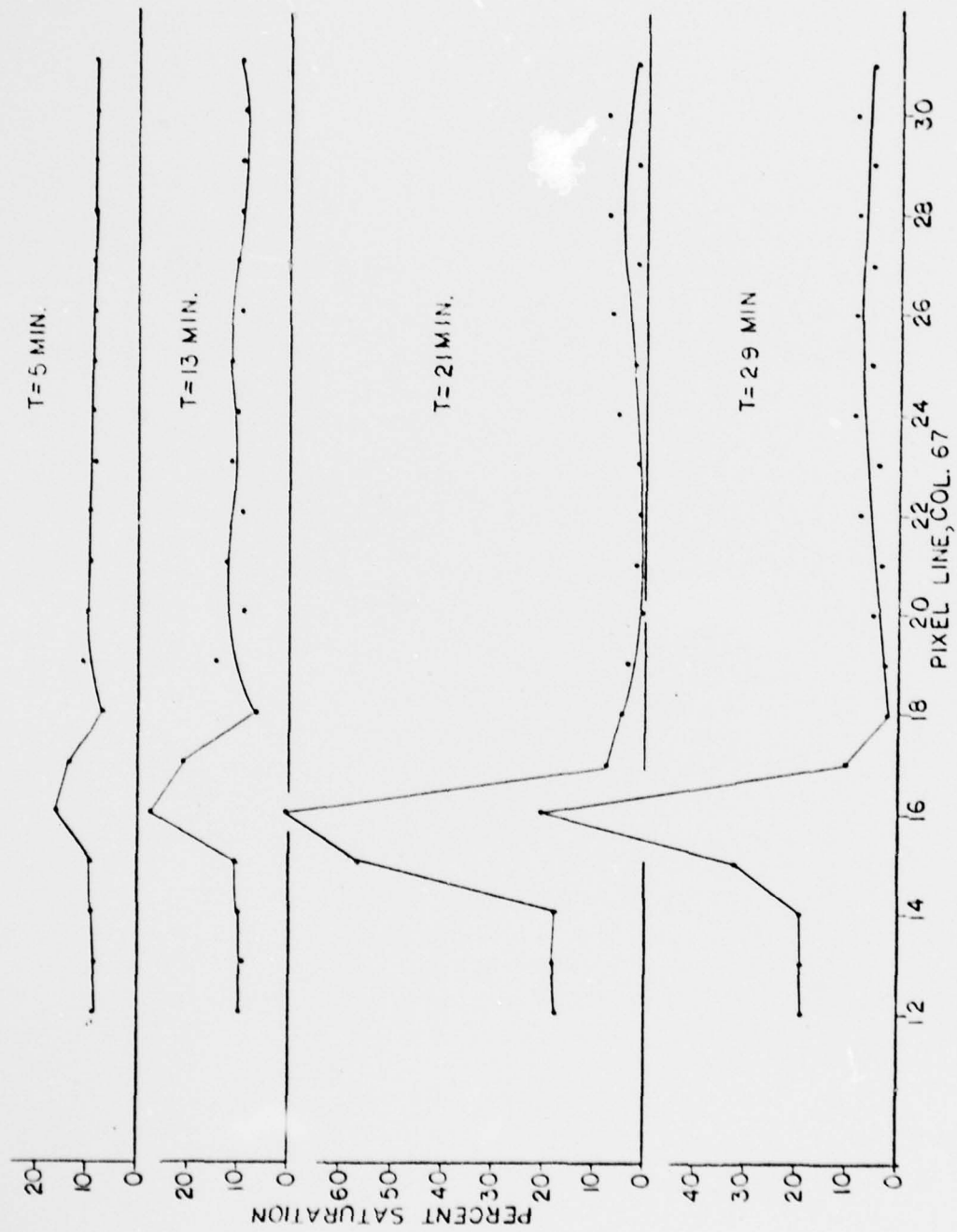


Figure 32. COLLATERAL DAMAGE: COLUMN 67 LEAKAGE CURRENT; 18 keV, 0°C

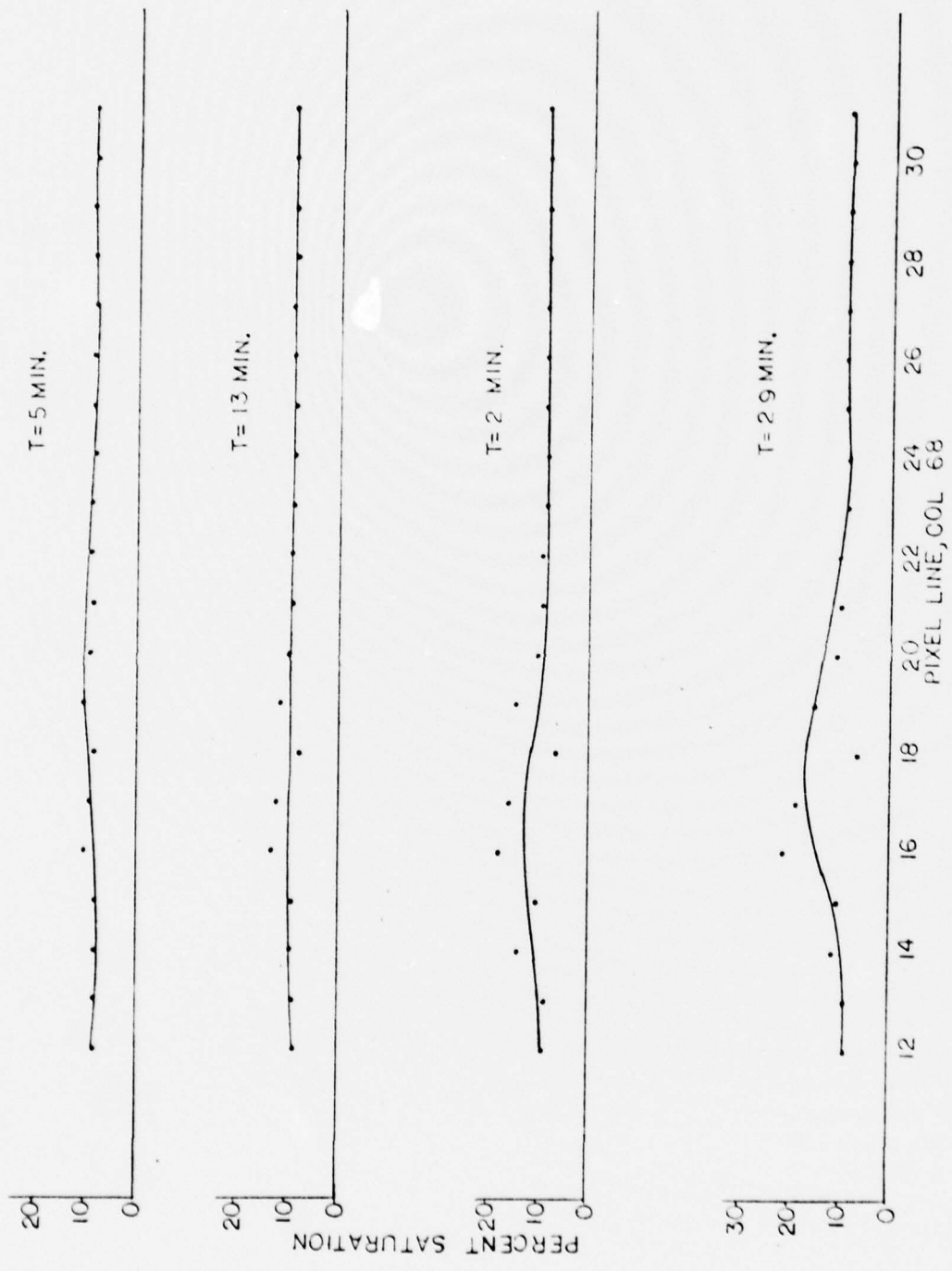


Figure 33. COLLATERAL DAMAGE: COLUMN 68 LEAKAGE CURRENT;
18 keV, 0°C

		COLUMN								
		65	66	67	65	66	67	65	66	67
Lines	14	-1	6	2	3	1	7	-2	-1	2
	15	3	4	2	1	0	3	-1	-2	15
	16	3	6	5	1	1	5	1	4	0
	17	4	13	9	1	7	2	2	9	3
	18	18	61	49	2	44	0	8	25	-5
	19	35	132	67	20	76	3	12	3	5
	20	29	92	48	16	66	10	7	50	7
	21	10	34	15	11	30	1	8	16	4
	22	9	6	3	3	4	11	2	5	3
	23	2	3	2	2	2	3	1	7	4
T=0		0	-1	2	3	3	4	4	0	0
		-2	3	2	4	3	13	0	4	0
		5	9	8	8	9	0	4	8	3
		6	22	19	9	50	4	6	10	6
		16	90	81	14	40	8	7	13	2
		20	130	67	16	50	0	5	8	8
		13	47	32	9	25	3	4	48	10
		6	16	7	3	10	5	1	6	2
		3	6	5	-2	1	2	1	6	1
		-1	2	0	5	4	2	1	5	3
T=5 MIN. LINE		-1	1	1	-1	-2	3			
		2	3	2	1	0	5			
		1	6	5	4	4	0			
		7	21	65	4	8	13			
		18	62	5	9	7	0			
		28	136	61	13	0	3			
		14	68	27	21	76	0			
		9	29	7	6	25	2			
		6	12	7	1	11	-2			
		3	0	1	1	3	2			
T=9 MIN.										
T=13 MIN.										
T=17 MIN.										
T=21 MIN.										
T=25 MIN.										
T=29 MIN.										

Figure 34. VARIATION OF SPOT CONTOUR DURING TEST

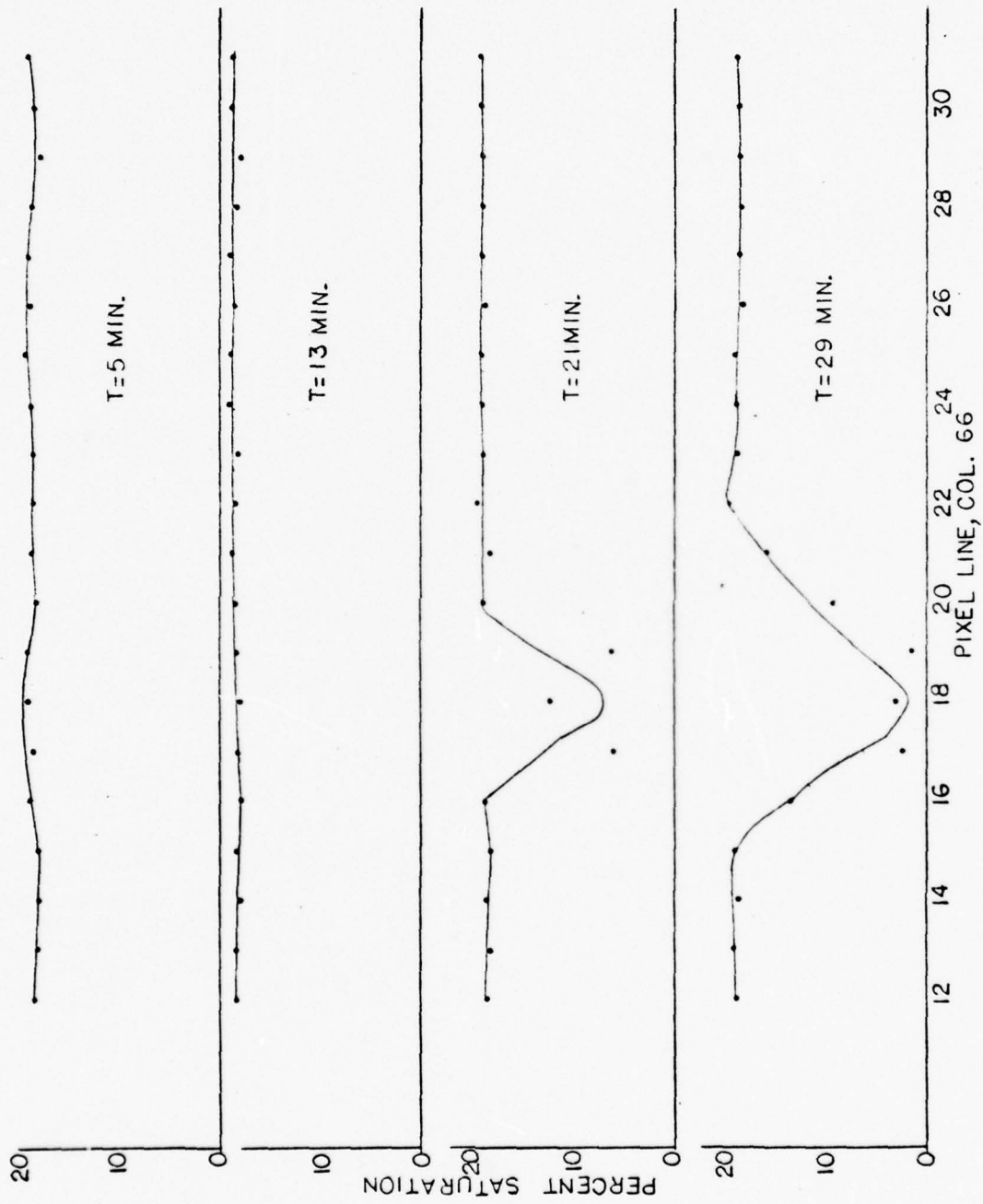


Figure 35. COLLATERAL DAMAGE: COLUMN 66 RESPONSE TO VISIBLE LIGHT;
18 keV, 0°C

signal for each pixel in column 66 for the same four points in time as were used in Figure 31.

In the region indicated by the electron spot, typical electron damage occurred. The leakage currents for pixels not within the electron spot but in the same columns as irradiated pixels (both above and below the irradiated pixels) increased slightly. No significant effects were apparent for pixels in other columns. The responsivity of pixels within the spot decreased as expected; however, no significant change in responsivity was observed for pixels outside of the spot, even in columns which intersected the spot.

2.4 Thermal Annealing of Electron Damaged CCD

Thermal annealing was attempted on the CCD202 unit after electron damage. Recovery (reduction of the leakage current) on the electron-damaged pixels was partial; recovery of a corona discharge-damaged region was nearly complete. The data are presented in Figure 36.

The array was subjected to a total of one hour at 200°C and four hours at 300°C in a vacuum. There was no observable change in leakage current or responsivity of the array after one hour at 200°C. The data presented here are the initial condition and following (a) 1 hours at 200°C and 2 hours at 300°C, and (b) 1 hour at 200°C and 4 hours at 300°C.

The video line signal plots show the dark current of each pixel (excepting line-end pixels) for line 54. This line passes through the region of peak electron-induced damage. The zero level, pixel dark signal, and saturation level are shown

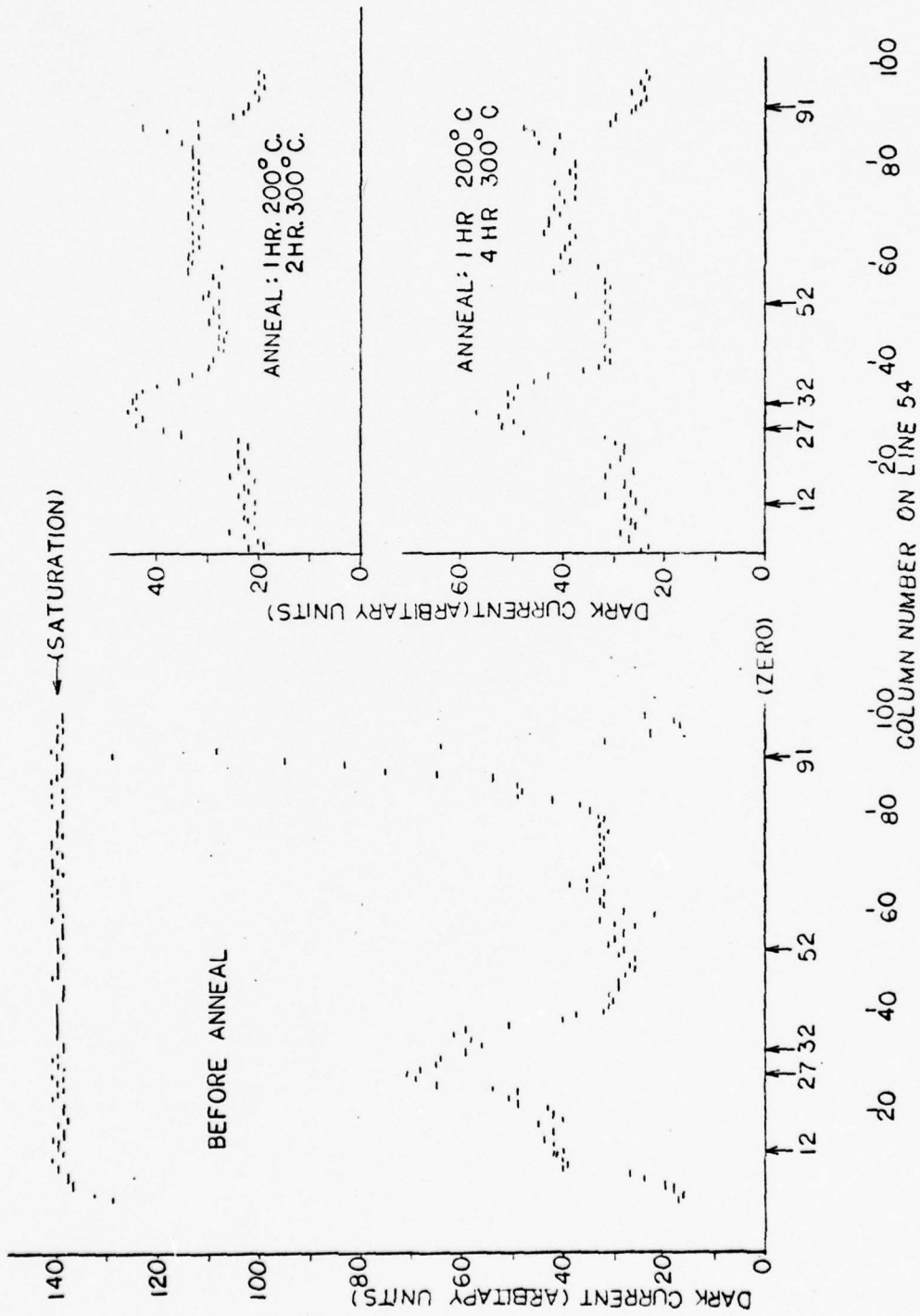


Figure 36. LEAKAGE CURRENT LINE 54 EFFECT OF THERMAL ANNEALING

on each graph. The abscissa is the pixel (column) number and the ordinate is the amplitude of the dark current signal in arbitrary units.

Five pixels in line 54 are chosen for analysis

Column 12: undamaged area

Column 27: electron damaged area (used for damage tests)

Column 32: electron damaged "dead" area (used for damage tests)

Column 52: undamaged area

Column 91: corona damaged area (accidentally damaged by glow discharge in vacuum system)

The location of these pixels are marked on Figure 36 for convenience.

As seen by comparison of the curves, the leakage current signals of the electron damaged regions were reduced by annealing but not to the levels of the adjacent undamaged regions. The dark signal of the corona-damaged region was reduced dramatically.

In addition, upon annealing the responsivity to visible light generally decreased, with the exception of the "dead" region which increased slightly. The "dead" region showed some responsivity to light even before annealing began.

The CCD202 was operated for these tests at clock voltages different from those in use at the end of the tests during which the electron damage occurred. This was required because the CCD202 will not now operate properly at those damage test voltages. In addition, before annealing and at the present voltages, the electron damaged region appeared reduced from its dark

signal level at the completion of the damage tests; the reason for this is not known, but may be due to some slight annealing at room temperature.

Annealing at higher temperatures was not attempted as the array was damaged during the last thermal cycle. This caused higher than normal heat dissipation in the array during operation and made intercomparison of the leakage current measurements difficult.

Annealing of an electron-damaged array by the use of intense ultraviolet light and by low energy electrons was also attempted on the electron-damaged array, but with no success. A description of these tests follows.

With the accelerating voltage and all array voltages turned off, the array was exposed to intense ultraviolet light from a 100 watt mercury arc lamp for periods of 10 and 15 minutes. No change was seen in the leakage current.

Using the low power mercury discharge lamp and the microprojector, the array (with no operating voltages applied) was subjected to 10 keV photoelectrons for 185 seconds. At turn-on (after irradiation) the array appeared to be dead, but it slowly recovered sensitivity after about five minutes. No improvement in the leakage current was seen. The test was repeated at 8 kV with similar effect and results. A third repetition (10 kV) in which the array was left off overnight before checking also gave no positive results.

Lastly, the energy of the photoelectrons was scanned from 18 keV to 2 keV in 2 keV increments with 15 seconds dwell at each level (array off). Again, no improvement resulted.

With the exception of some positive results in the initial thermal-vacuum attempts, no annealing of the electron beam induced leakage current was observed. Annealing procedures involving higher temperatures or longer times might prove to be effective but were not attempted in this program. Even if successful, such procedures would not be practical for extending the lifetime of an ICCD tube.

3.0 SURVEY OF OTHER CCD DAMAGE DATA

3.1 Introduction

The feasibility of detecting low-level light signals using an electron bombarded charge coupled device (ICCD) has drastically increased detector sensitivity for UV and visible photometry. However, the electron bombardment of CCDs limits detector lifetime because of electron damage to the CCD array.

The effects of space and nuclear radiation on metal-oxide-semiconductor configuration type electronic/optical devices has been extensively studied and documented (2) since the mid-1960s. The effect of ionizing radiation causes buildup of charges in the oxide layer, and increases the density of states at the oxide-silicon interface. These mechanisms adversely affect the operation of MOS-type electronic/optical devices including ICCDs. In the space and nuclear radiation environment, hardening technology has been developed which permits hardness levels of 10^7 rads (Si) in contrast to the 10^4 rads (Si) levels for unhardened devices.

The radiation damage mechanisms for operating ICCDs are identical to damage mechanisms produced by space and nuclear weapon radiation environments. The only difference is that the radiation environments are different in particle type, energy, dose, and dose rate. However, if the mechanisms are understood there should be no problem in interpolating from one radiation environment to another.

3.2 Basic Mechanisms

One of the earliest basic studies of low energy electron damage to MOS devices was the work of Simons.⁽²⁾

From this work it can be concluded that:

1. There is charge buildup in the oxide layers of MOS samples.
2. This charge buildup is a function of the beam energy dissipated in the oxide in the vicinity of the oxide-silicon interface.
3. Charge buildup is a function of electron energy due to range-energy relationships.
4. This charge buildup can be thermally annealed at 300°C for 5 to 10 minutes.

Subsequent work has shown that MOS device operation is degraded by radiation due to this charge buildup.

3.3 Front Surface Illumination

Front surface illuminated CCDs have been evaluated for radiation effects by at least three groups. The work of Currie (U. of Md.),⁽³⁾ Ginaven and Choisser (EVC)⁽⁴⁾ and Cheng (LLL)⁽⁶⁾ studied the electron damage to Fairchild CCD201, 202 and 211 arrays. These studies produce similar and, at times, confusing data. However, the data generally show an increase in dark current and decreases in responsivities as a function of 6 and 15 kV electron fluence. At fluence levels of 10^6 to 10^7 electrons/pixel, the pixels died (responsivity went to zero): with a pixel area of $5.4 \times 10^{-6} \text{ cm}^2$ the electron fluence at each pixel at death is about 2×10^{12} electrons/cm²,

corresponding to a dose of about 5×10^4 rads (Si). This is in agreement with radiation damage basic mechanisms studies,⁽¹⁾ in which unhardened oxides fail at about 10^4 rads (Si).

From the front side measurements, it appears that for typical operating conditions the life of front side illuminated CCDs would be only tens of hours, as will be shown in Section 4.0. If present day hardening technology⁽⁵⁾ is applied to the CCDs, it should be possible to obtain a factor of 10-100 increase in lifetime which would correspond to operating lifetimes of the order of 100 to 1000 hours.

3.4 Back Side Illumination

Since the effect of electron irradiation on a CCD depends on the dose deposited in the oxide layer, it appears that back side illumination of the CCD, where the dose is deposited in the substrate before reaching the semiconductor-oxide interface, will provide radiation hardening. Borsak⁽⁷⁾ electron irradiated thinned back side illuminated CCDs from Texas Instruments at 8 kV and 20 kV. Their results showed that upon irradiation the dark current increased slightly while the responsivity decreased and eventually went to zero. Pixel death occurred at approximately 3×10^{10} electrons/pixel. This is a factor of about 10^4 higher than front side illuminated ICCDs.

Similarly, Cheng (LLL)⁽⁶⁾ irradiated thinned back side illuminated RCA CCDs at 6 kV and did not see any changes in the dark current or responsivity for the length of their irradiation. Cheng feels that thinned back irradiated CCDs provide at least a factor of 10^3 hardening over front irradiated CCDs. Caldwell

and Boyle (NVL)⁽⁸⁾ mentioned no degradation of their thinned back side illuminated CCD from Texas Instruments in a set of experiments. General Electric⁽⁹⁾ in using thinned back illuminated CIDs reported no electron damage during the course of their experiments.

It appears clear that thinned back side illuminated CCDs provide hardening to electron irradiation damage compared with front side illuminated CCDs.

With a minimal hardening factor of 10^3 in using thinned back side illuminated CCDs instead of front side illuminated CCDs, the operating lifetime of an ICCD can be extended to the order of 10^4 hours. Furthermore, if hardened oxides with back side illuminated CCDs are used, the lifetime could be extended to the order of 10^6 hours.

4.0 LIFETIME ASSESSMENT AND CONCLUSIONS

The primary objective of this study has been the investigation of possible methods of extending the lifetime of front irradiated (Fairchild CCD202) intensified charge-coupled device detectors for space applications.

Measurements of pixel dark current, electron sensitivity, and light sensitivity have been made as a function of electron fluence at electron energies of 18 keV and 15 keV with the array at room temperature and at 18 keV with the array at 0°C. Severe increases in dark current and reduction in electron sensitivity were observed at electron fluences between 10^6 and 10^7 electrons per pixel. In addition to damage within the electron spot, vertical streaking occurred at very high electron fluences.

In an effort to extend the lifetime of front irradiated ICCDs, parameter studies of the effects of electron energy, temperature of operation of the ICCD, clock voltage, pixel-to-pixel variations, and thermal and radiation annealing were performed.

Even though there were slight trends in the amount of damage as a function of electron energy (15 keV vs. 18 keV), temperature of ICCD (25°C vs. 0°C) and clock voltages, the improvements were insignificant in extending the lifetime of the front irradiated ICCD. In a similar manner, thermal (up to 300°C) and ionization annealing showed little promise for extending lifetime.

In order to estimate the useful lifetime of an ICCD, a total integrated count of 10^6 photoelectrons per pixel was assumed. The average count rate (photoelectrons per pixel per second) was estimated as follows.

During normal operation, an ICCD would receive signals from several sources. With adequate protection against viewing bright objects (such as the sun and moon) the most important sources of light are the zodiacal light and integrated starlight.

The zodiacal light is a bright sky background produced by sunlight scattering off of dust particles. The brightness of the zodiacal light as a function of solar elongation angle and ecliptic latitude, as given by Allen,⁽¹⁰⁾ was used to calculate the count rate of photoelectrons per pixel per second. This count rate is shown in Figure 37 for ecliptic latitudes of 0° and 30°. In the plane of the ecliptic, the zodiacal light is a strong function of solar angle, producing a count rate of about 2000 photoelectrons per second per pixel at about 10 degrees from the sun. This calculation was performed for an ICCD containing a Farichild CCD202 array and a S-20 photocathode at the focal plane of a 73 mm focal length telescope with a 4.62 cm² collecting aperture.

The average pixel count rate due to integrated starlight, again calculated using data compiled by Allen,⁽¹⁰⁾ is shown in Figure 38. This count rate is significant only near the galactic plane where it reaches a value of about 23 photoelectrons per second per pixel.

The exact value of the pixel count rate will depend on the solar angle, ecliptic latitude and galactic latitude of the area of sky viewed by the detector. Estimates of the average count rate may be made from the zodiacal light and integrated starlight

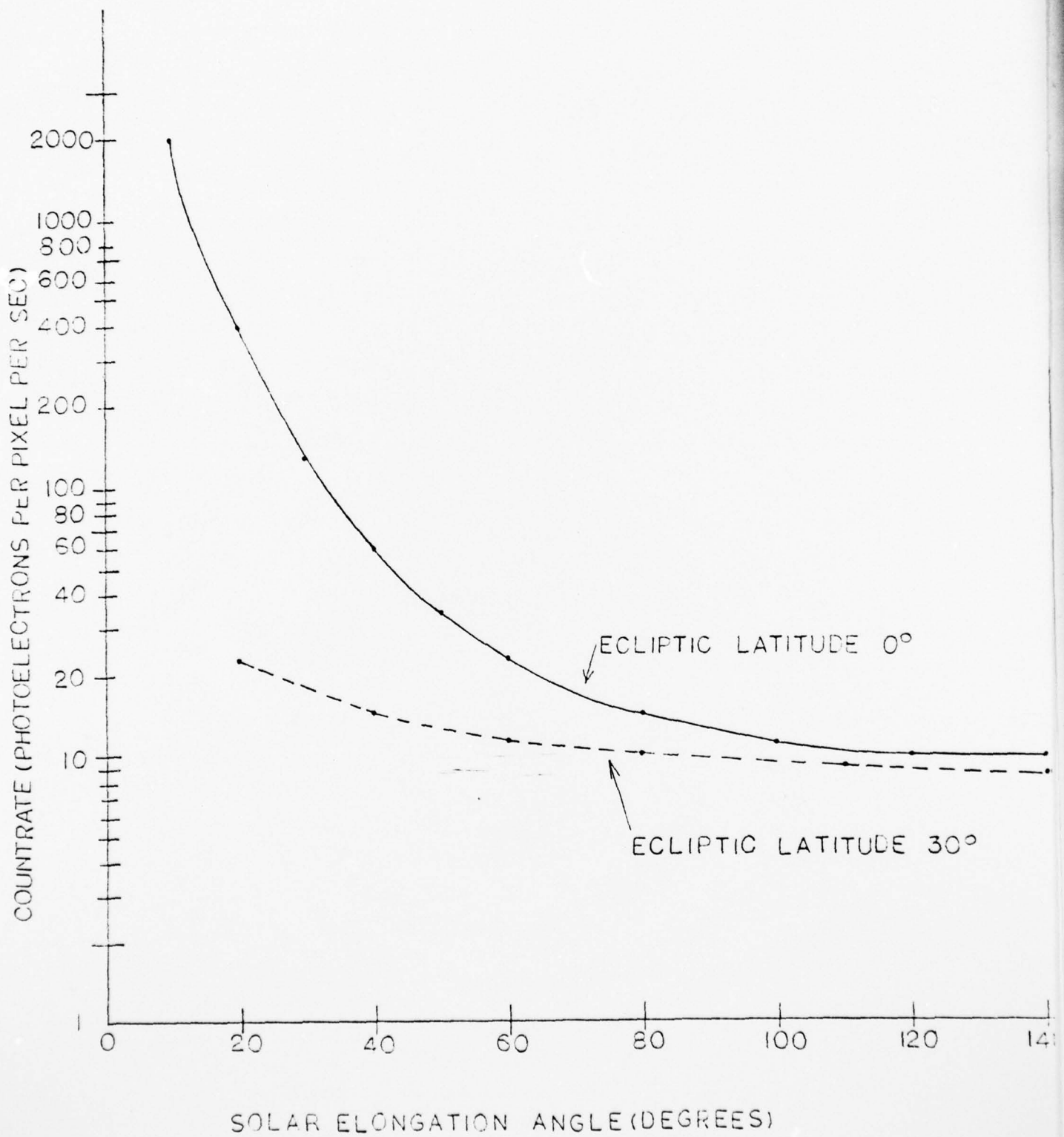


Figure 37. COUNT RATE PER PIXEL FROM ZODIACAL LIGHT

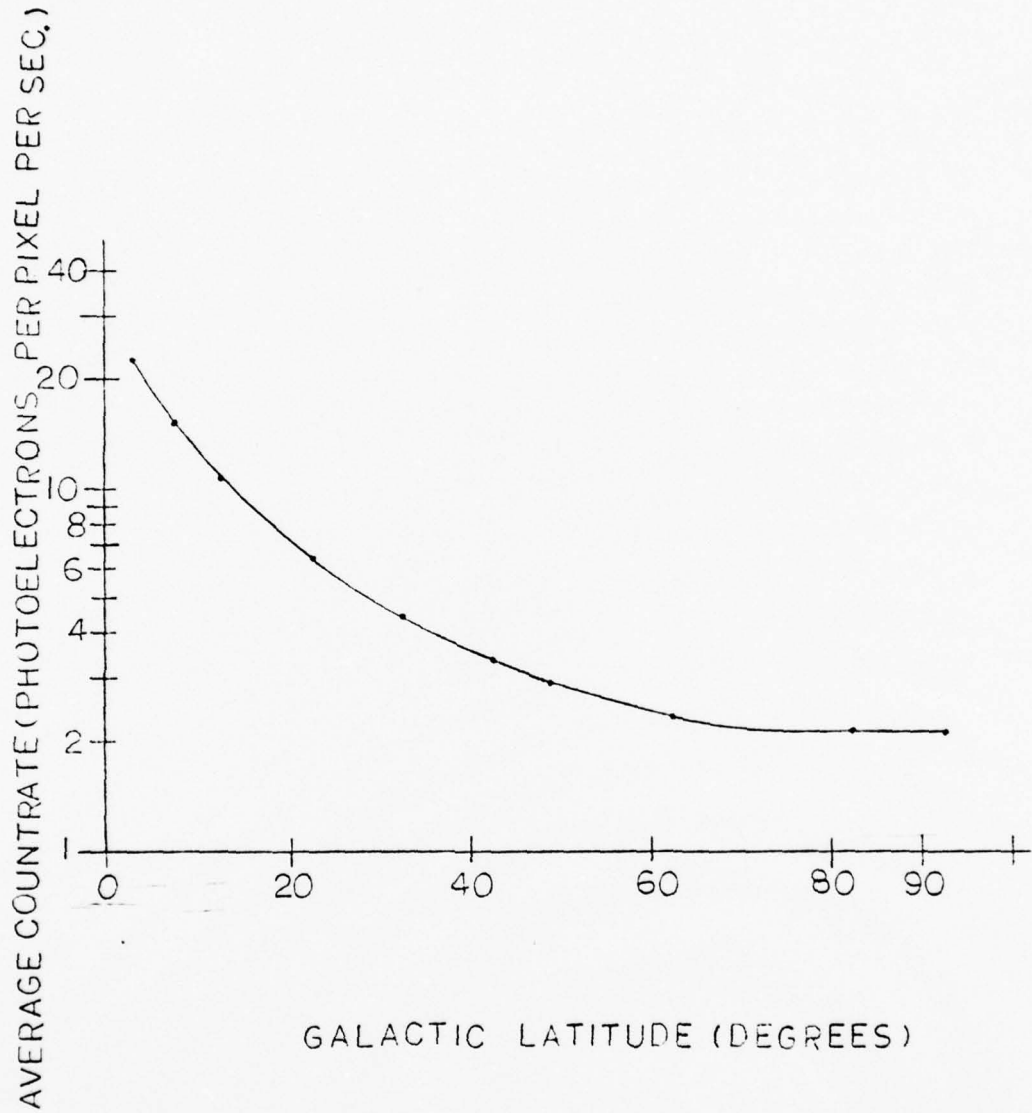


Figure 38. COUNT RATE PER PIXEL FROM INTEGRATED STARLIGHT

intensities, noting that it is unlikely that the sensor field of view will be in both the ecliptic plane and the galactic plane. From Figures 37 and 38, it is apparent that over most of the sky the pixel count rate should be below 30 photoelectrons per second which corresponds to a detector lifetime (10^6 electrons) of approximately 10 hours. However, operating in the plane of the ecliptic at solar angles of less than 60 degrees would significantly shorten the detector lifetime. For example, a lifetime of about one hour would be expected at a solar angle of 20 degrees (in the plane of the ecliptic).

The detector lifetime would be reduced even more drastically by exposure to bright objects such as the sun, moon and earth. Obviously, any very sensitive detector would have to be protected against such exposures.

From the present study, the only technique that could significantly extend the lifetime of the present version of the front-illuminated Fairchild CCD202 appears to be to sequentially utilize different areas of the CCD as the array is damaged. This is possible because no significant horizontal blooming of the damaged region was observed. Possibly the use of a rectangular aperture in the optical system could protect unused portions of the array for later use. This aperture could then be shifted to a fresh area when leakage currents began to exceed a predetermined value. By using different groups of columns the lifetime could be extended by possibly a factor of ten for normal operation. Also, it would preclude the detector being blinded by a single overexposure, except when the last good segment is in operation.

The use of radiation hardening techniques in the fabrication of the array may be able to extend the lifetime of a front-illuminated CCD by a factor of 100. While this effect is insufficient by itself to produce an adequate lifetime, used in conjunction with other techniques (such as segmenting the array or backside-illumination) it might provide an added safety margin.

The technique that shows the most promise for significantly extending the CCD lifetime is the use of thinned rear-illuminated CCDs. While the availability of such arrays continues to be a problem, they do promise an increase in lifetime by a factor of 1000 or more over the front-illuminated CCDs.

REFERENCES

1. H. Borke, IEEE Transaction on Nuclear Science, NS-24.2043, December 1977.
2. M. Simons, et al, IEEE Transactions on Electron Devices, November 1968.
3. D. G. Currie, Proceedings of Conference on Charge Coupled Device Technology and Applications, November 1976.
4. J. P. Choisser, Proceedings of Conference on Charge Coupled Device Technology and Applications, November 1976.
5. C. P. Chang and K. G. Aubuchon, CCD Radiation Hardening, Hughes Aircraft Company Report No. P77-125, Final Report on Naval Research Laboratory Contract No. N00173-76-C-0166, March, 1977.
6. J. Cheng of Lawrence Livermore Laboratories, Private Communication.
7. G. M. Borsak, et al, Proceedings of Conference on Charged Coupled Device Technology and Applications, November 1976.
8. L. Caldwell and J. Boyle, SPIE Low Light Level Devices, 78, 10, 1976.
9. Private Communication
10. C. W. Allen, Astrophysical Quantities, Third Edition, Athone Press, London, 1973.

PRIMARY DISTRIBUTION LIST

Defense Documentation Center (DDC) Cameron Station Alexandria, VA 22314	12
Air University Library Maxwell AFB, AL 36112	1
HQ AFSC/DLCEA Andrews AFB, MD 20334 Attn: Dr. F. Jenkins	1
HQ AF/RDSD Washington, DC 20330 Attn: LtCol Bracken	1
AFAL/WRA-1 Library Wright-Patterson AFB, OH 45433 Attn: B. J. Sabo	1
AFAL/WRA Wright-Patterson AFB, OH 45433 Attn: LtCol Duggins	1
The Aerospace Corporation P O Box 92957 Worldway Postal Center Los Angeles, CA 90009 Attn: Dr. J. Reinheimer	1
Dr. S. Kash	2
N. C. Chang	1
R. B. Wood	1
R. F. Cannata	1
HQ SAMSO P O Box 92960 Worldway Postal Center Los Angeles, CA 90009 Attn: Col Randolph (YN)	1
Capt Turnipseed (YNV)	1



ELECTRONIC VISION COMPANY
A Division of Science Applications, Inc.

11526 Sorrento Valley Road
San Diego, California 92121 (714) 453-2870

